Remote Sensing of Environment 117 (2012) 34–49

Contents lists available at SciVerse ScienceDirect

Remote Sensing of Environment

journal homepage: www.elsevier.com/locate/rse

Remote sensing of impervious surfaces in the urban areas: Requirements, methods, and trends

Qihao Weng *

Center for Urban and Environmental Change, Department of Earth and Environmental Systems, Indiana State University, Terre Haute, IN 47809, USA

ARTICLE INFO

Article history:
Received 20 November 2010
Received in revised form 17 February 2011
Accepted 27 February 2011
Available online 1 September 2011

Keywords:
Urban remote sensing
Impervious surfaces
Remotely sensed data characteristics
Urban mapping requirements
Pixel-based algorithms
Sub-pixel based algorithms
Object-oriented method
Artificial neural networks

ABSTRACT

The knowledge of impervious surfaces, especially the magnitude, location, geometry, spatial pattern of impervious surfaces and the perviousness–imperviousness ratio, is significant to a range of issues and themes in environmental science central to global environmental change and human–environment interactions. Impervious surface data is important for urban planning and environmental and resources management. Therefore, remote sensing of impervious surfaces in the urban areas has recently attracted unprecedented attention. In this paper, various digital remote sensing approaches to extract and estimate impervious surfaces will be examined. Discussions will focus on the mapping requirements of urban impervious surfaces. In particular, the impacts of spatial, geometric, spectral, and temporal resolutions on the estimation and mapping will be addressed, so will be the selection of an appropriate estimation method based on remotely sensed data characteristics. This literature review suggests that major approaches over the past decade include pixel-based (image classification, regression, *etc.*), sub-pixel based (linear spectral unmixing, imperviousness as the complement of vegetation fraction *etc.*), object-oriented algorithms, and artificial neural networks. Techniques, such as data/image fusion, expert systems, and contextual classification methods, have also been explored. The majority of research efforts have been made for mapping urban landscapes at various scales and on the spatial resolution requirements of such mapping. In contrast, there is less interest in spectral and geometric properties of impervious surfaces. More researches are also needed to better understand temporal resolution, change and evolution of impervious surfaces over time, and temporal requirements for urban mapping. It is suggested that the models, methods, and image analysis algorithms in urban remote sensing have been largely developed for the imagery of medium resolution (10–100 m). The advent of high spatial resolution satellite images, spaceborne hyperspectral images, and LiDAR data is stimulating new research idea, and is driving the future research trends with new models and algorithms.
© 2011 Elsevier Inc. All rights reserved.

1. Introduction

Impervious surfaces are anthropogenic features through which water cannot infiltrate into the soil, such as roads, driveways, sidewalks, parking lots, rooftops, and so on. In recent years, impervious surface has emerged not only as an indicator of the degree of urbanization, but also a major indicator of environmental quality (Arnold & Gibbons, 1996). Impervious surface is a unifying theme for all participants at all watershed scales, including planners, engineers, landscape architects, scientists, social scientists, local officials, and others (Schueler, 1994). The magnitude, location, geometry and spatial pattern of impervious surfaces, and the pervious–impervious ratio in a watershed have hydrological impacts. Although land use zoning emphasizes roof-related impervious surfaces, transport-related impervious surfaces could have a greater impact. The increase of impervious cover would lead to the increase in the volume, duration, and intensity of urban runoff (Weng, 2001). Watersheds with large amounts of impervious cover may experience an overall decrease of groundwater recharge and baseflow and an increase of stormflow and flood frequency (Brun & Band, 2000). Furthermore, imperviousness is related to the water quality of a drainage basin and its receiving streams, lakes, and ponds. Increase in impervious cover and runoff directly impact the transport of non-point source pollutants including pathogens, nutrients, toxic contaminants, and sediment (Hurd & Civco, 2004). Increases in runoff volume and discharge rates, in conjunction with non-point source pollution, will inevitably alter in-stream and riparian habitats, and the loss of some critical aquatic habits (Gillies et al., 2003). In addition, the areal extent and spatial occurrence of impervious surfaces may significantly influence urban climate by altering sensible and latent heat fluxes within the urban canopy and boundary layers (Yang et al., 2003). As impervious cover increases within a watershed/administrative unit, vegetation cover would decrease. The percentage of land covered by impervious surfaces varies significantly with land use categories and sub-categories (Soil Conservation Service, 1975).

* Tel.: +1 812 237 2255; fax: +1 812 237 8029.
E-mail address: qweng@indstate.edu.

0034-4257/$ – see front matter © 2011 Elsevier Inc. All rights reserved.
doi:10.1016/j.rse.2011.02.030

Therefore, estimating and mapping impervious surface is significant to a range of issues and themes in environmental science central to global environmental change and human–environment interactions. The datasets of impervious surfaces are valuable not only for environmental management, *e.g.*, water quality assessment and storm water taxation, but also for urban planning, *e.g.*, building infrastructure and sustainable urban development.

Many techniques have been applied to characterize and quantify impervious surfaces using either ground measurements or remotely sensed data. Field survey with GPS, although expensive and time-consuming, can provide reliable information on impervious surfaces. Manual digitizing from hard-copy maps or remote sensing imagery (especially aerial photographs) have also been used for mapping imperviousness. Later, this technique has become more heavily involved with automation methods such as scanning and the use of feature extraction algorithms. From the 1970s to 1980s, satellite imagery started to gain popularity in natural resources and environmental studies, and was used in the interpretive applications, spectral applications, and modeling applications of impervious surfaces (Slonecker et al., 2001). In reviewing the methods of impervious surface mapping, Brabec et al. (2002) identified four different approaches, *i.e.*, using a planimeter to measure impervious surface on aerial photography, counting the number of intersections on the overlain grid on an aerial photography, conducting image classification, and estimating impervious surface coverage through the percentage of urbanization in a region. These reviews concluded that in the 1970s and 1980s, aerial photography was the main source of remote sensing data for estimating and mapping impervious surfaces (Brabec et al., 2002; Slonecker et al., 2001).

A literature search via Scopus, the largest abstract and citation database of peer-reviewed literature, indicates that in the 1990s the number of publications on remote sensing of impervious surface was limited (Fig. 1). This is largely due to the lack of remote sensors suitable for detecting and estimating various types of impervious surfaces, immature digital image processing techniques, and constrained computing power. Then, at the turn of the 21st century, remote sensing of impervious surfaces was rapidly gaining interest in the remote sensing community. Fig. 1 shows that annual publications and citations on the subject increased exponentially. The average annual citation (number of citation per article per year) on remote sensing of impervious surfaces was 0.82 between 2001 and 2010, while the number of citations per year for the whole field of remote sensing was 0.55 for the same period. This comparison indicates that remote sensing of impervious surfaces has become one of the more dynamic fields in remote sensing. All major remote sensing journals in the world have published articles on this subject. Table 1 lists most relevant peer-refereed journals, along with most prolific authors and major research groups. Several factors contribute to the increase of the literatures and their significance. The advent of high-resolution imagery, especially those less than 5 m resolution, and more capable image processing techniques, have both driven the technologic advance in remote sensing of impervious surfaces. Driven by the concerns over global environmental change, societal needs of impervious surface data, and enhanced computing and internet technology, many municipal government agencies and non-government organizations have started to collect and map impervious surface data for civil and environmental uses. Given increasing importance in the field of remote sensing, it becomes an urgent need to systematically examine the current state of the research and to trace its future trends. This review begins with examining data requirements for remote sensing of impervious surfaces, with a particular interest in the impacts of remotely sensed data characteristics (*i.e.*, spatial, spectral, and temporal resolutions, and LiDAR data). Next, various digital methods for extracting and estimating impervious surfaces are assessed. In addition, the author will address future developments by looking into how emerging algorithms in digital image processing will influence the field of remote sensing in general and impervious surfaces estimation and mapping in particular.

2. Remote sensing data considerations

2.1. Spatial resolution

Spatial resolution is a function of sensor altitude, detector size, focal size and system configuration (Jensen, 2005). It defines the level of spatial detail depicted in an image, and it is often related to the size of the smallest possible feature that can be detected from an image. This definition implies that only objects larger than the spatial resolution of a sensor can be picked out from an image. However, a smaller feature may sometimes be detectable if its reflectance dominates within a particular resolution cell or it has a unique shape (*e.g.*, linear features). Another meaning of spatial resolution is that a ground feature should be distinguishable as a separate entity in the image. But the separation from neighbors or background is not always sufficient to identify the object. Therefore, the concept of spatial resolution includes both detectability and separability. For any feature to be resolvable in an image, it involves consideration spatial resolution, spectral contrast, and as well as feature shape. Jensen and Cowen (1999) suggested that the minimum spatial

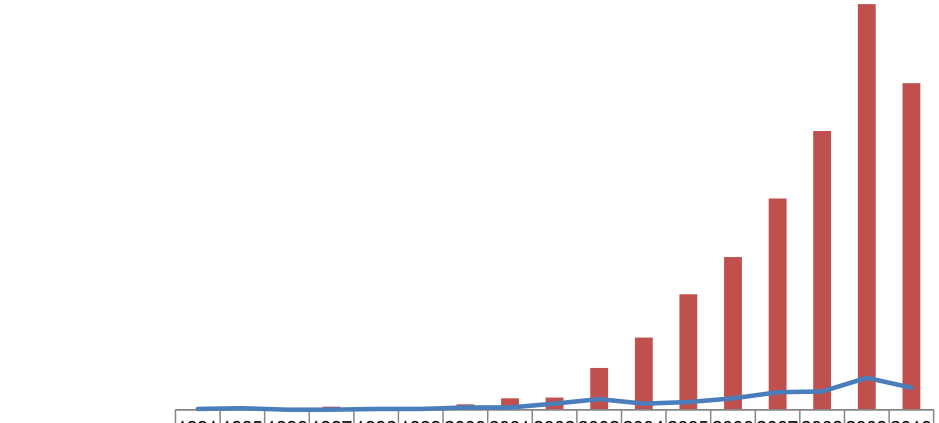

	1991	1995	1996	1997	1998	1999	2000	2001	2002	2003	2004	2005	2006	2007	2008	2009	2010
# citations	0	0	1	4	1	1	7	15	16	55	95	152	201	278	367	534	430
# publications	1	2	0	0	1	1	3	3	8	14	8	10	15	23	24	42	29

Fig. 1. Yearly publications and citations from 1991 to 2000 indexed by Scopus. The search was conducted on February 16, 2011, and found a total of 184 articles (including journal articles and those published in conference proceedings). Total number of citation yielded 2157, but Scopus does not have complete citation information for articles published before 1996.

Table 1
Literature search results using Scopus on "remote sensing impervious surface".

Most relevant journals (# of publications)	Most prolific authors (# of publications on the subject)	Major research groups
Photogrammetric Engineering & Remote Sensing (22)	Weng, Q. (14)	USGS/Earth Resources Observation and Science Center/SAIC (17)
Remote Sensing of Environment (18)	Lu, D. (7)	Indiana State University (16)
International Journal of Remote Sensing (18)	Wu, C. (7)	Univ. of Wisconsin Milwaukee (8)
Canadian Journal of Remote Sensing (6)	Xian, G. (7)	Indiana University (6)
IEEE Transactions on Geoscience and Remote Sensing (4)	Murray, A.T. (5)	University of Utah (5)
Journal of the American Water Resources Association (4)	Yang, L. (5)	Minnesota State University (5)
Water Science and Technology (3)	Yuan, F. (5)	Chinese Univ. of Hong Kong (4)
Sensors (3)	Carlson, T.N. (4)	NASA Goddard Space Flight Center (4)
ISPRS Journal of Photogrammetry and Remote Sensing (2)	Bauer, M.E. (4)	Hohai University (4)
International Journal of Applied Earth Observation and Geoinformation (2)	Hu, X. (4)	Chinese Academy of Sciences (4)
GIScience and Remote Sensing (2)	Crane, M. (4)	United States EPA (4)
Geocarto International (2)	Jiang, L. (4)	Wuhan University (4)
Computers Environment and Urban Systems (2)	Liao, M. (3)	University of Minnesota (4)
Journal of Hydrology (2)	Goetz, S.J. (3)	Zhejiang Forestry University (4)
Journal of Applied Meteorology and Climatology (2)	Ridd, M.K. (3)	
Acta Ecologica Sinica (2)	Imhoff, M.L. (3)	
IAHS AISH Publication (2)	Bounoua, L. (3)	

Note: The search was conducted on October 14, 2010. In addition to journal articles, conference proceedings have also published on the subject, *e.g.*, Proceedings of SPIE (14), IGARSS (12), 2009 Joint Urban Remote Sensing Event in Shanghai (9), and 2007 Joint Urban Remote Sensing Event in Paris (2).

resolution requirement should be one-half the diameter of the smallest object of interest. For two major types of impervious surface, buildings (perimeter, area, height, and property line) and roads (width) are generally detectable with the minimum spatial resolution of 0.25 to 0.5 m, while road centerline can be detected at a lower resolution of 1–30 m (Jensen & Cowen, 1999). Before 1999, lack of high spatial resolution (less than 10 m) images is a main reason for scarce research in remote sensing of impervious surfaces before 2000. Cracknell (1999) asserted that NOAA's AVHRR had been the major instrument for remote sensing studies between 1980 and 1999, and that Landsat or SPOT was not mentioned among the 12 most cited papers published in the International Journal of Remote Sensing during this period. The medium (10–100 m) spatial resolution images, such as Landsat and SPOT, were not readily available and were expensive. Many researchers employed per-pixel classifiers and applied successful experience in vegetation mapping to remote sensing of impervious surfaces (Bauer et al., 2004; Carlson, 2004; Gillies et al., 2003). This approach can avoid a major problem that existed in the medium resolution imagery, *i.e.*, mixed pixels.

Mixed pixels dominate in coarse resolution images such as AVHRR and MODIS. However, for a remote sensing project, image spatial resolution is not the only factor needed to consider. The relationship between the geographical scale of a study area and the spatial resolution of remote sensing image has to be studied (Quattrochi & Goodchild, 1997). For mapping at the continental or global scale, coarse spatial resolution data are usually employed. Gamba and Herold (2009) assessed eight major research efforts in global urban extent mapping, and found that most maps were produced at the spatial resolution of 1–2 km. When using coarse resolution images, a threshold has to be defined with respect to what constitute a built-up/impervious pixel (Lu et al., 2008; Schneider et al., 2010). Reliable impervious surface data that derive from medium resolution imagery are helpful for validating and predicting urban/built-up extent at the coarse resolution level (Lu et al., 2008).

With the advent of very high resolution satellite imagery, such as IKONOS (launched 1999), QuickBird (2001), and OrbView (2003) images, great efforts have been made in the applications of these remote sensing images in urban and environmental studies. High resolution satellite imagery has been applied in impervious surface mapping (Cablk & Minor, 2003; Goetz et al., 2003; Hu & Weng, 2011; Lu & Weng, 2009; Wu, 2009). These fine spatial resolution images contain rich spatial information, providing a greater potential to extract much more detailed thematic information (*e.g.*, land use and land cover), cartographic features (buildings and roads), and metric information with stereo-images (*e.g.*, height and area). These information and cartographic characteristics are highly beneficial to estimating and mapping of impervious surfaces. The proportion of mixed pixels is significantly reduced in an image scene. However, some new problems come with these image data, notably shadows caused by topography, tall buildings, or trees (Dare, 2005), and the high spectral variation within the same land cover class (Hsieh et al., 2001). Shadows obscure impervious surfaces underneath and thus increase the difficulty to extract both thematic and cartographic information. These disadvantages may lower image classification accuracy if classifiers used cannot effectively handle them (Cushnie, 1987; Irons et al., 1985). In order to make full use of the rich spatial information inherent in fine spatial resolution data, it is necessary to minimize the negative impact of high intra-spectral variation. Algorithms that use the combined spectral and spatial information may be especially effective for impervious surface extraction in the urban areas (Lu & Weng, 2007).

2.2. Geometric characteristics of urban features

Urban surface geometry has an important impact in remote sensing based analysis in general and impervious surface estimation in particular. High spatial resolution image data, including both space-borne and airborne, provide a great possibility to achieve the effectiveness and efficiency of extraction of cartographic features (*e.g.*, building, roads, and parking lots) through automated extraction methods. But the issues of shadow and image distortion can affect the extraction accuracy to a certain degree. Because urban streets were misclassified as vegetation, it may lead to 30% of error, generally an underestimation of impervious surface estimation in the urban areas (van der Linden & Hostert, 2009). In contrast, Hodgson et al. (2003) found that the low reflectance from pixels under shadow frequently resulted in a misclassification into the water class. Displaced buildings may occlude adjacent non-building impervious surfaces. The confusion between them, as a function of building height and view-angle, may add up to 16% error to the final impervious surface map compared to nadir regions (Linden and Hostert, 2009). The issue of viewing angle is also pertinent to space-borne sensors such as IKONOS and QuickBird, which also provide off-nadir imagery at view-angles of up to 30°. Zhou and Kelmelis (2006) presented a protocol of three steps for orthophoto generation, aiming at 3-D city modeling. These steps included: digital terrain model based- and digital building model based-orthoimage generation, and their merging. This protocol is capable of shadow

detection and restoration, as well as occlusion detection and compensation (Zhou & Kelmelis, 2006). Tong et al. (2009) suggested that high resolution satellite imagery, such as QuickBird, must be accurately ortho-rectified by using the principle of photogrammetry before applying for mapping of urban land use.

LiDAR data has been increasingly used in many geospatial applications due to its high data resolution, short processing time, and low cost. Unlike other remotely sensed data, LiDAR data focus solely on geometry rather than radiometry. Feature classification and extraction based on LiDAR data have been widely conducted (Clode et al., 2007; Filin, 2004; Forlani et al., 2006; Lee et al., 2008), and LiDAR data have shown a great potential in building and road extraction because of elevation data can be derived quickly and at high resolution in comparison to photogrammetric techniques (Miliaresis & Kokkas, 2007). In addition, some researchers have used LiDAR in conjunction with optical remote sensing data in impervious surface estimation and mapping. Hodgson et al. (2003), for example, used both digital aerial photographs and LiDAR data for urban parcel impervious surface mapping, and found that the combined datasets improved the results for all classification approaches over the color aerial photography. The addition of height information from LiDAR increased the coefficient of determination value by 2% to 25%.

Building extraction is a feature classification and detection, as well as a pattern recognition technique. Aerial imagery is a popular data source for building extraction due to its high spatial resolution. An important prerequisite is the number of images in which a scene can be found. Mono, stereo, and multi-spectral images can be distinguished and used in reconstruction of objects (Mayer, 1999). Multiple views of observation enable a better geometry reconstruction of building objects and reduce the problems with occlusion. Multispectral high-resolution satellite imagery such as Quickbird and IKONOS are regarded as a repeatable data source for building extraction with a stereo-viewing capacity and a short revisit time (1 to 3.5 days for Quickbird, 3 to 5 days for IKONOS). LiDAR data provide a unique data source and has advantages over satellite imagery and aerial photographs in accurate capturing of urban features with absolute height information, especially for building extraction (Yu et al., 2010).

A wide range of models and methods have been developed for building extraction. Most of the extraction algorithms use edge-based techniques that consist of linear feature detection for perpendicular outline and flat roof, grouping for parallelogram structure hypothesis extraction, and building polygons verification using knowledge such as geometric structure, shadows and walls, illuminating angles, substructures like doors or windows, and so forth (Jin & Davis, 2005). These edge-based techniques mainly utilize the geometric properties of buildings, while other techniques are combined with consideration of image attributes at multiple scales. Apart from geometry, detailed image models with rich radiometric attributes can exploit much better information contained in the image (Braun et al., 1995; Henricsson, 1998; Lang & Forstner, 1996; Moons et al., 1998). With data fusion algorithms, both panchromatic and multi-spectral images from different sensors may be utilized (Henricsson, 1998; Moons et al., 1998). In addition, by assessing multiple scales, one can start with reliable structures in a coarse scale and then focus extraction on specific areas and object types in fine scales (Mayer, 1999).

Remote sensing research on road extraction from aerial or satellite images began in 1970s when only low- and medium-resolution imagery were available. Mena (2003) presented a comprehensive review on automatic road extraction, and grouped the methods/algorithms into six categories: road tracking, mathematical morphology, snake, knowledge-based, multi-resolution and multi-resource methods, and integrated systems. In low- and medium-resolution images, the road extraction was often considered as a linear feature extraction method, and roads as continuous and smooth lines (Amini et al., 2002). The extraction of roads as surfaces was applied to aerial images only (Peteri & Ranchin, 2007). The advent of high-resolution imagery expands the surface approach for extraction of roads. Many methods have been developed to detect urban road network from high-resolution images (Hu et al., 2007; Long & Zhao, 2005; Shi & Zhu, 2002; Zhu et al., 2005). High resolution imagery allows more fine details to be seen, a better differentiation of road types, and a more accurate geographic location. The geometric characteristics of ground features may also be detected. Geometric characteristics, such as structures and shapes, are very important in road recognition, so that roads can be modeled as continuous and elongated homogeneous regions with nearly constant width (Long & Zhao, 2005). The main limitations associated with road extraction include geometric noises caused by cars, ground markings, shadows, and so on, and these noises increased intra-class spectral variance. Both problems contribute to the difficulty of road extraction when the surface approach is applied, which assumes the homogeneity in radiometry along a road. Other problem relates to similar radiometry between road pixels and surrounding areas, such as builds and parking lots (Peteri & Ranchin, 2007). In this regard, elevation information can be very useful to reduce the ambiguity between roads and the backgrounds. Because LiDAR data can provide height, shape and other geometric information, it has been increasingly employed in road extraction. Clode et al. (2004) used a hierarchical classification technique to classify LiDAR points into road and non-road, and obtained an acceptable quality of 0.62. Clode et al. (2005) proposed a region growing algorithm to detect the road network in Fairfield and Yeronga, Australia. Samadzadegan et al. (2009) presented an optimum multiple classifier system for classification and extraction of road objects, in which both height and intensity information of LIDAR data was used. The method was applied to the city of Castrop-Rauxel in the west of Germany. In some recent studies, LiDAR data is combined with other types of data to improve the extraction accuracy. Elberink and Vosselman (2009) used airborne laser data fused with topographic map data to build an automated method for 3D modeling of highway interchanges in the Netherlands, and achieved an average precision of 10 to 15 cm. Tiwari et al. (2009) explored an integrated approach to extract road automatically using airborne laser scanning altimetry and high-resolution data. This method was applied to Amsterdam, The Netherlands, and yielded accuracy over 90%.

2.3. Spectral resolution

Remote sensing of impervious surfaces should consider the requirements for mapping three interrelated entities or substances on the Earth surface (*i.e.*, material, land cover, and land use) and their relationships. Mapping of each entity/substance must consider the spectral resolution of a remote sensor. The spectral features include the number, locations, and bandwidths of spectral bands. The number of spectral bands can range from a limited number of multispectral bands (*e.g.*, 4 bands in SPOT data and 7 for Landsat TM), to a medium number of multispectral bands (*e.g.*, ASTER with 14 bands and MODIS with 36 bands), and to hyperspectral data (*e.g.*, AVIRIS and EO-1 Hyperion images with 224 bands). A large number of spectral bands provide the potential to derive detailed information on the nature and properties of different surface materials on the ground, but it also means a difficulty in image processing and a large data redundancy due to high correlation among the adjacent bands. Increase of spectral bands may improve classification accuracy, only when those bands are useful in discriminating the classes (Thenkabail et al., 2004a).

Urban areas are composed of a variety of materials, including different types of artificial materials (*i.e.*, impervious surfaces), soils, rocks and minerals, green and non-photosynthetic vegetation. These materials comprise land cover, and are used in different manners for various purposes by human beings. Land cover can be defined as the biophysical state of the earth's surface and immediate subsurface, including biota, soil, topography, surface and ground water, and human structures (Turner et al., 1995). Land use can be defined as the human use of the land, and involves both the manner in which the biophysical attributes of the land are manipulated and the purpose for which the

land is used (Turner et al., 1995). Remote sensing technology has often been applied to map land use or land cover, instead of materials. Each type of land cover may possess unique surface properties (material), however, mapping land covers and materials have different requirements (Fig. 2). Land cover mapping needs to consider characteristics in addition to those coming from the material (Herold et al., 2006). The surface structure (roughness) may influence the spectral response as much as the intra-class variability (Gong & Howarth, 1990; Herold et al., 2006; Myint, 2001; Shaban & Dikshit, 2001). Two different land covers, for example, asphalt roads and composite shingle/tar roofs, may have very similar materials (hydrocarbons) and thus are difficult to discern, although from a material perspective, these surfaces can be mapped accurately with hyperspectral remote sensing techniques (Herold et al., 2006). Therefore, land cover mapping requires taking into account of the intra-class variability and spectral separability. On the other hand, analysis of land use classes would nearly be impossible with spectral information alone. Additional information, such as spatial, textural, and contextual information, is usually required in order to have a successful land use classification in urban areas (Gong & Howarth, 1992; Herold et al., 2003; Stuckens et al., 2000).

Linear spectral mixture analysis (LSMA) has been widely used in impervious surface estimation, implying that impervious surface is a type of surface material. This view has much to do with the spectral resolution of a remote sensor. LSMA is a physically deterministic modeling method that decomposes the signal measured at a given pixel into its component parts called endmembers (Adams et al., 1986; Boardman, 1993; Boardman et al., 1995). Endmembers are regarded as recognizable surface materials that have homogenous spectral properties all over the image. Impervious surfaces can be extracted and mapped as a single endmember, or the combination of two or more end-members (Lu & Weng, 2006; Rashed et al., 2003; Weng et al., 2008, 2009; Wu & Murray, 2003). Previous research has largely applied LSMA to medium spatial resolution, multi-spectral images, such as Landsat TM/ETM+ and Terra's ASTER images, for extraction of impervious surfaces (Weng, 2007). However, both spatial and spectral resolution is regarded as too coarse for use in urban environments because of the heterogeneity and complexity of urban impervious surface materials. In the LSMA model, the maximum number of endmembers is directly proportional to the number of spectral bands used. Hyperspectral imagery may be more effective in extracting endmembers than multispectral imagery. The vastly increased dimensionality of a hyperspectral sensor may remove the sensor-related limit on the number of endmembers available. More significantly, the fact that the number of hyperspectral image channels far exceeds the likely number of endmembers for most applications readily permits the exclusion from the analysis of any bands with low signal-to-noise ratios or with significant atmospheric absorption effects (Lillesand et al., 2004). In previous research, hyperspectral data have been successfully used for land use/cover classification (Benediktsson et al., 1995; Hoffbeck & Landgrebe, 1996; Platt & Goetz, 2004; Thenkabail et al., 2004a,b), vegetation mapping (McGwire et al., 2000; Pu et al., 2008; Schmidt et al., 2004), and water mapping (Bagheri & Yu, 2008; Moses et al., 2009). As space-borne hyperspectral data such as EO-1 Hyperion become available, research and applications with hyperspectral data will increase. Weng et al. (2008) found a Hyperion image was more powerful in discerning low albedo surface materials, which has been a major obstacle for impervious surface estimation with medium resolution multispectral images. A sensitivity analysis suggested that the improvement of mapping accuracy in general and the better ability in discriminating low albedo surfaces resulted largely from additional bands in the mid-infrared region (Weng et al., 2008).

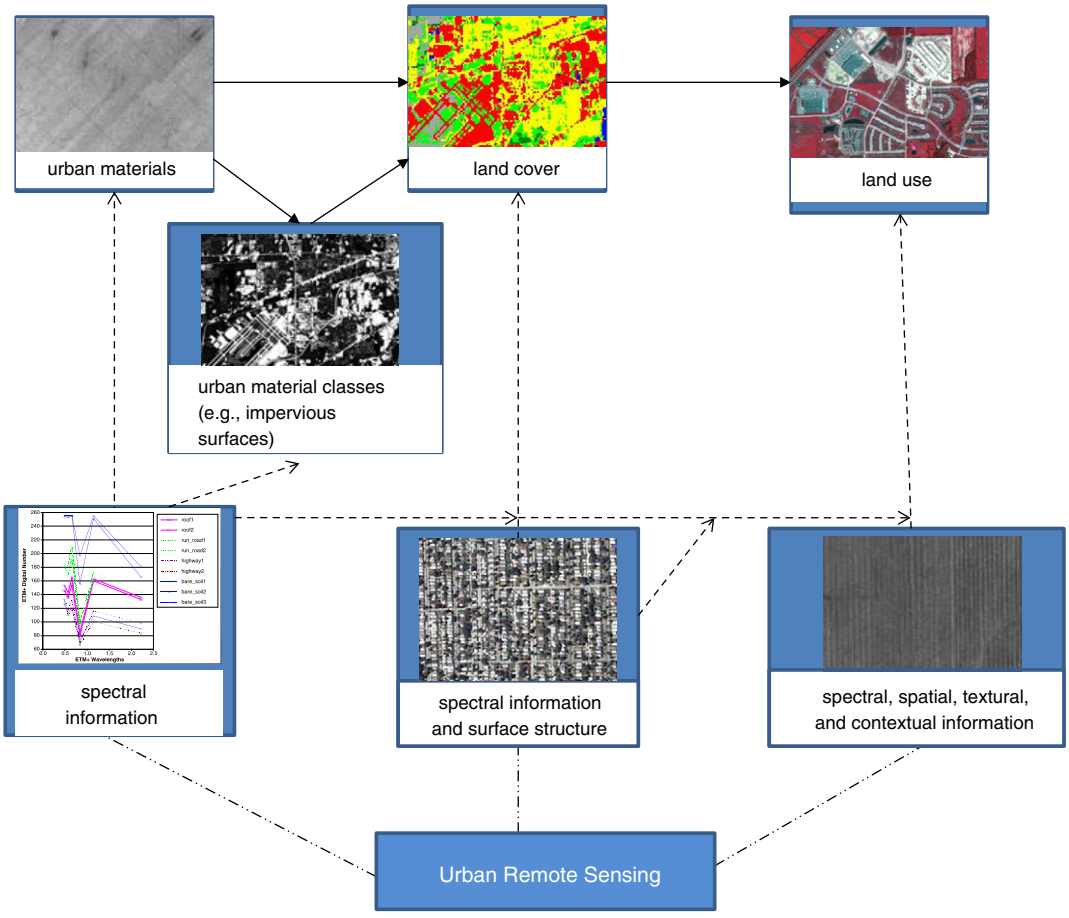

Fig. 2. Illustration of the relationship among remote sensing of urban materials, land cover, and land use (after Weng & Lu, 2009).

The spectral characteristics of land surfaces are the fundamental principles for land imaging. Previous studies have examined the spectral properties of urban materials (Ben-Dor et al., 2001; Heiden et al., 2007; Hepner et al., 1998; Herold et al., 2003) and spectral resolution requirements for separating them (Jensen & Cowen, 1999). When Jensen and Cowen (1999) explained minimum spectral resolution requirements for urban mapping, the discussion focused mainly on multispectral imagery data. They suggested that spatial resolution was more important than spectral resolution in urban mapping. The spectrum from visible to NIR, MIR, and microwave are suitable for LULC classification at coarser categorical resolutions (*e.g.*, Levels I and II of the Anderson classification); however, at the finer categorical resolutions (*e.g.*, Levels III and IV of the Anderson classification) and for extraction of buildings and roads, panchromatic band is needed (Jensen & Cowen, 1999). Other urban studies had employed hyperspectral sensing for discriminating among urban surface features based on their diagnostic absorption and reflection characteristics and for detailed identification of urban materials. Hepner et al. (1998) suggested that IFSAR imagery, when combined with AVIRIS data, can provide information on 3D geometry, topography, and impervious surfaces, and other urban surface characteristics. Ben-Dor et al. (2001) examined the feasibility of using detailed spectral information in the spectral region of 0.4–1.1 μm for identifying different features in the urban environment using Compact Airborne Spectral Imager (CASI) data. Herold et al. (2003) found that several bands in the visible, NIR and SWIR regions were best suited for distinguishing different urban features, and emphasized that both reflection and absorption features due to material composition in the SWIR region was significant in urban land cover classification, especially in separating different types of impervious surfaces. Heiden et al. (2007) presented a hierarchical classification method for the derivation of diagnostic urban spectral features that can be used for an automated identification of spectrally homogeneous endmembers from hyperspectral image data.

2.4. Temporal resolution

Temporal resolution refers to the amount of time it takes for a sensor to return to a previously imaged location, commonly known as the repeat cycle or the time interval between acquisitions of two successive images. For air-borne remote sensing, temporal resolution is less pertinent, since users can schedule flights for themselves. Jensen and Cowen (1999) suggested that studies of urban development, buildings and property infrastructure, and road center lines only need to have an image every one to five years. They further suggested that the temporal resolution requirement should be a bit higher for delineating precise road width, namely, one to two years. However, Herold (2007) believed that road aging and deterioration may have various temporal resolution depending up on the quality of pavement, traffic, and distresses (*e.g.*, cracks and raveling).

Temporal differences between remotely sensed imagery are not only caused by the changes in spectral properties of the Earth's surface features/objects, they can also result from atmospheric differences and changes in sun position during the course of a day and during the year. Temporal resolution is a very important consideration in remote sensing of vegetation, because vegetation grows according to daily, seasonal, and annual phenological cycles. Weng et al. (2009) found that a summer ASTER image was better for estimation of impervious surfaces than a spring (April) and a fall (October) one based on a case study in Indianapolis, U.S.A. it is suggested that mapping of impervious surfaces tended to be more accurate with contrasting spectral response from green vegetation when LSMA technique was employed. Plant phenology caused changes in the variance partitioning and impacted the mixing space characterization, leading to a less accurate estimation of impervious surfaces in the spring and fall (Weng et al., 2009). When other methods are used, detection of urban buildings and roads may well be suited in the leaf-off season in the temperate regions. In addition, the set overpass times of satellites may coincide with clouds or poor weather conditions. This is especially true in the tropical and coastal areas, where persistent clouds and rains in the wet season offer limit clear views of the Earth's surface and thus prevent from getting good quality images (Lu et al., 2008). In consideration of the impact of street trees on impervious surfaces, Linden and Hostert (2009) suggested that the quantification of this impact was generally possible by performing multi-temporal analyses at leaf-on/leaf-off seasons, but solar illumination geometry and shadowing can presumably preclude leaf-off acquisitions for many temperate cities.

The off-nadir imaging capability of satellite sensors, such as SPOT-5, IKONOS and Quickbird, reduces the usual revisit time depending on the latitude of the imaged areas. This feature is designed for taking stereoscopic images and for producing digital elevation models, but it obviously also allows for more frequent coverage of selected regions for short periods, and provides another means for monitoring and assessing impervious surfaces.

3. Assessing the current state of the field

3.1. Major methods of estimation and mapping

Many factors must be taken into account in selecting an image processing method for use. Researchers may have to consider the user's need, research objectives, remotely sensed data available, compatibility with previous work, availability of image processing algorithms and computer software, and time constraints (Lu & Weng, 2007). Among these factors, the selection of suitable remote sensing data is the first important step for a successful application (Jensen & Cowen, 1999; Phinn, 1998; Phinn et al., 2000). The data selection closely relates to research purposes and requirement, the scale and characteristics of a study area, the analyst's understanding of image data and their characteristics, cost and time constraints. Since remotely sensed data vary in spatial, geometric, radiometric, spectral, and temporal resolutions, complete understanding of the strength and weakness of various types of data is key to a proper data selection. A review of the literature on remote sensing of impervious surfaces over the past decade shows that spatial resolution of remotely sensed data is an important consideration in the selection of image processing methods to be used (Table 2).

Because of the near inverse correlation between impervious surface and vegetation cover in urban areas, one potential approach for impervious surface extraction is through information on vegetation distribution (Bauer et al., 2007; Carlson & Arthur, 2000; Gillies et al., 2003). The Normalized Difference Vegetation Index (NDVI) or greenness from tasseled cap transformation or principal component analysis may be utilized to represent vegetation distribution. Vegetation fractional coverage can then be computed from a scaled NDVI (Carlson & Ripley, 1997; Gillies et al., 1997). Impervious surfaces are estimated based on: (1) complement of vegetation fraction; or (2) regression models with vegetation indices. The first method is largely applied to coarse- and medium-resolution satellite imagery, such as AVHRR imagery in Carlson and Arthur (2000), MODIS NDVI imagery in Boegh et al. (2009), Landsat MSS imagery in Gillies et al. (2003) and TM imagery in Carlson (2004). This approach drew rich experiences in remote sensing of vegetation and hydroclimate studies, and has the merit of be simplistic. This approach, however, has a major drawback. Different seasons of satellite images could result in large variations in impervious surface estimation. In the leaf-on season, vegetation may be considerably overestimated, while in the leaf-off season, vegetation tends to be underestimated, leading to the overestimation of impervious surface coverage. By developing a regression modeling method, Bauer et al. (2004, 2007) related impervious surface area delineated from panchromatic digital orthophoto quadrangles to Landsat tasseled cap derived greenness to estimate and map the impervious surface in the state Minnesota.

Table 2
Selected literature in remote sensing of urban impervious surfaces.

Data spatial resolution	Sensor type	Techniques used	References
Low (>100 m)	MODIS NDVI	Regression, complement of vegetation fraction,	Lu et al., 2008; Boegh et al., 2009
	AVHRR	Complement of vegetation fraction	Carlson & Arthur, 2000
	DMSP-OLS	Regression	Elvidge et al., 2007; Lu et al., 2008
Medium (10–100 m)	Landsat MSS	Complement of vegetation fraction, LSMA/rule-based classification, expert system	Gillies et al., 2003; Powell et al., 2008; Elmore & Guinn, 2010
	Landsat TM	SubPixel classifier (Erdas Imagine), regression, complement of vegetation fraction, LSMA	Civco et al., 2002; Carlson, 2004; Bauer et al., 2007; Yuan et al., 2008
	Landsat ETM+	SubPixel classifier (Erdas Imagine), CART, LSMA, ANN, MESMA	Civco et al., 2002; Yang et al., 2003; Wu & Murray, 2003; Lu & Weng, 2006; Lee & Lathrop, 2006; Powell et al., 2007
	ASTER	LSMA, ANN	Weng & Hu, 2008; Hu & Weng, 2009; Weng et al., 2009
	SPOT	CART, object-based	Yang et al., 2009; Tan et al., 2009
High (<10 m)	IKONOS	PCA/morphological operators, ANN, decision tree, LSMA, MLC	Cablk & Minor, 2003; Lu & Weng, 2009; Mohapatra and Wu, 2007
	QuickBird	Multiple agent segmentation and classification, object-based, hybrid classification	Lu et al., in press; Yuan & Bauer, 2006; Zhou and Wang, 2008
Airborne Data	HyMap	SVM	Linden and Hostert, 2009
	Digitized color orthophoto-graph	MLC, spectral clustering, expert systems	Hodgson et al., 2003
	1:50,000 aerial photograph	Manual interpretation	Phinn et al., 2002

Note: PCA — principal component analysis; ANN — artificial neural network; LSMA — linear spectral mixture analysis; MLC — maximum likelihood classifier; CART — classification and regression tree; MESMA — multiple endmember spectral mixture analysis; SVM — support vector machine.

The regression analysis has further been conducted by Chabaeva et al. (2004) and Yuan et al. (2008), which developed a land use based estimation model. Yang et al. (2003) extended the regression method by developing a classification and regression tree (CART) algorithm, which used the classification result of high resolution imagery as the raining dataset to generate a rule-based modeling for prediction of sub-pixel percent imperviousness for a large area. Regression trees were constructed using a partitioning algorithm that built a tree by recursively splitting the training sample into smaller subsets, aiming at reducing the model's combined residual error for the subsets. Xian (2007) maintained that an advantage of the regression tree algorithm was to simplify complicated non-linear relationship between predictive and target variables into a multivariate linear relation and to accept both continuous and discrete variables as input data for continuous variable prediction. In addition to medium resolution imagery data, the regression approach has also been applied to coarse resolution imagery, such as MODIS NDVI (Lu et al., 2008) and DMSP-OLS (Elvidge et al., 2007). These studies employed a similar approach, which usually used finer resolution data for calibration and validation, and predicted impervious surface area at the regional or continental levels by using coarser resolution data. Whether multivariate regression or CART, the estimation of impervious surfaces using regression methods has to consider major limitations related to model calibration, validation, and extrapolation of the models to other study areas.

As indicated by Table 2, LSMA is another main approach for remote sensing of impervious surfaces with medium resolution imagery. As a physically based image analysis procedure, LSMA supports repeatable and accurate extraction of quantitative sub-pixel information (Roberts et al., 1998a). Because of its effectiveness in handling spectral mixture problem, LSMA has been widely used in estimation of impervious surfaces in recent years (Lu & Weng, 2006; Madhavan et al., 2001; Phinn et al., 2002; Powell et al., 2007; Ward et al., 2000; Weng et al., 2008, 2009; Wu & Murray, 2003; Yang et al., 2009). Different algorithms of impervious surface extraction based on the LSMA model have been developed. The straightforward method is that impervious surface was extracted as one of the endmembers in the standard SMA model (Phinn et al., 2002). Impervious surface estimation can also be done by the addition of high-albedo and low-albedo fraction images, with both as the endmembers (Lu & Weng, 2006; Weng et al., 2008, 2009; Wu & Murray, 2003). However, these LSMA based methods share a common problem, that is, impervious surface tends to be overestimated in the areas with small amounts of impervious surface, but is underestimated in the areas with large amounts of impervious surface. The similarity in spectral properties among non-photosynthetic vegetation, soil, and various impervious surface materials makes it difficult to distinguish impervious from pervious materials. In addition, shadows caused by tall buildings and large tree crowns in the urban areas may lead to underestimation of impervious surface area with high resolution imagery.

Generally speaking, urban areas have substantially different impervious surfaces in terms of types, abundance and geometry. Identifying one suitable endmember to represent all types of impervious surfaces is often found problematic. Lu and Weng (2004) suggested that three possible approaches may be taken to overcome these problems by: (1) stratification, (2) use of multiple endmembers, and (3) use of hyperspectral imagery. The multiple endmember SMA (MESMA) method has been developed by Rashed et al. (2003), Powell et al. (2007), and Franke et al. (2009). This approach starts with a series of candidate two-endmember models and then evaluates each model based on the criteria of fraction values, root mean square error, and residual threshold, and finally produces fraction images with the lowest error (Roberts et al., 1998b). Another problem with LSMA is the end member selection associated with within-class spectral variability (Foody et al., 1997). To overcome this problem, Wu (2004) improved his method of impervious surface estimation by normalizing spectral data before applying LSMA, and found normalized spectral mixture analysis (NSMA) useful. Yang et al. (2010) presented a pre-screened and normalized multiple endmember spectral mixture analysis (PNMESMA) method, which combined NSMA and MESMA. The PNMESMA method was found superior to the previous methods (LSMA, NSMA, LSMA-LST, and MESMA) in that the estimation error (overall root mean square error) was reduced to 5.2%, and no obvious underestimation or overestimation occurred for high or low impervious surface areas.

Image classification is one of the widely used methods in extraction of impervious surfaces (Dougherty et al., 2004; Hodgson et al., 2003; Jennings et al., 2004), but results are often not satisfactory because of the limitation of spatial resolution in medium resolution imagery and the heterogeneity of urban landscapes. Various impervious surfaces may be intermingled with other land cover types, such as trees, grasses, and soils. Moreover, the difficulty in selecting training areas could also affect the accuracy of image classification. As fine spatial resolution data (especially better than 5 m in spatial resolution), such as IKONOS and

QuickBird, become available, they are increasingly employed for different applications including impervious surface mapping. A major advantage of these images is that such data greatly reduce the mixed pixel problem, providing a greater potential to extract more detailed information on land covers (Hsieh et al., 2001). Therefore, traditional image classification methods, based on the image color and tone, have been employed in a number of studies (Lu et al., in press; Lu & Weng, 2009; Zhou & Wang, 2008). In the meantime, other important information rich in high resolution imagery, such as texture, shape, and context, should also be utilized (Sharma & Sarkar, 1998). An interesting use with these high resolution images is to separate dark impervious surface areas and shadowed impervious surfaces from water and shaded areas created by tree crowns (Lu & Weng, 2009). They also demonstrated that a hybrid approach based on a decision tree classifier and an unsupervised ISODATA classifier can effectively extract impervious surfaces from IKONOS images, and provided a significantly better result than the maximum likelihood classifier. Image classification has been applied to aerial photographs and LIDAR data too. Hodgson et al. (2003) compared the performance of per-pixel maximum likelihood classifier, ISODATA, and a rule-based classification algorithm applied to digitized aerial photos and LiDAR data (2×2 m posting) in Richland County, South Carolina, and found the maximum likelihood classifier yielded the highest accuracy while the ISODATA the lowest accuracy.

3.2. The per-pixel vs. sub-pixel debate

Per-pixel classifiers typically develop a signature by combining the spectra of all training set pixels for a given feature. The resulting signature contains the contributions of all materials present in the training pixels, but ignoring the impact of the mixed pixels. Per-pixel based classification algorithms may be parametric or nonparametric. The parametric classifiers assume that a normally distributed dataset exists, and that the statistical parameters generated from the training samples are representative. However, the assumption of normal spectral distribution is often violated, especially with complex landscapes such as urban areas. In addition, insufficient, non-representative, or multimode distributed training samples can further introduce uncertainty in the image classification procedure (Lu & Weng, 2007). The maximum likelihood is a well-known parametric classifier because of its availability in any image processing software. With nonparametric classifiers, the assumption of a normal distribution of dataset is not required. No statistical parameters are needed to develop for separating image classes. Nonparametric classifiers are thus especially suitable for the incorporation of non-spectral data into a classification procedure. Much previous research has indicated that nonparametric classifiers may provide better classification results than parametric classifiers in complex landscapes (Paola & Schowengerdt, 1995). Among the most commonly used nonparametric classifiers are artificial neural network, decision tree classifier, support vector machine, and expert systems. However, the variation in the dimensionality of a dataset and the characteristics of training and testing sets may lessen the accuracy of image classification (Foody & Arora, 1997). Bagging, boosting, or a hybrid of both techniques may be used to improve classification performance in a nonparametric classification procedure (Lu & Weng, 2007). These techniques have been used in decision tree (DeFries & Chan, 2000; Lawrence et al., 2004) and support vector machine (Kim et al., 2003) to enhance classification results.

Per-pixel classifications prevail in the previous remote sensing literature, in which each pixel is assigned to one category and land cover (or other themes) classes are mutually exclusive. Per-pixel classification algorithms are sometimes referred to as "hard" classifiers. Due to the heterogeneity of landscapes (particularly in urban landscapes) and the limitation in spatial resolution of remote sensing imagery, mixed pixels are common in medium and coarse spatial resolution data. The presence of mixed pixels has been recognized as a major problem, affecting the effective use of per-pixel classifiers (Cracknell, 1998; Fisher, 1997). The mixed pixel problem results from the fact that the scale of observation (*i.e.*, spatial resolution) fails to correspond to the spatial characteristics of the target (Mather, 1999). Strahler et al. (1986) defined H- and L-resolution scene models based on the relationship between the size of the scene elements and the resolution cell of the sensor. The scene elements in the L-resolution model are smaller than the resolution cells, and are thus not detectable. When the objects in the scene become increasingly smaller than the resolution cell size, they may no longer be regarded as individual objects. Hence, the reflectance measured by the sensor may be treated as the sum of interactions among various types of scene elements as weighted by their relative proportions (Strahler et al., 1986). This is what happens with medium resolution imagery, such as those of Landsat TM or ETM+, ASTER, SPOT, and Indian satellites, applied for urban mapping. As the spatial resolution interacts with the fabric of urban landscapes, the problem of mixed pixels is created. Such a mixture becomes especially prevalent in residential areas where buildings, roads, trees, lawns, and water can all lump together into a single pixel (Epstein et al., 2002). The low accuracy of image classification in urban areas reflects, to a certain degree, the inability of traditional per-pixel classifiers to handle composite signatures. Therefore, the "soft" approach of image classifications has been developed, in which each pixel is assigned a class membership of each land cover type rather than a single label (Wang, 1990). Different approaches have been used to derive a soft classifier, including fuzzy set theory, Dempster–Shafer theory, certainty factor (Bloch, 1996), and neural network (Foody, 1999; Mannan & Ray, 2003). Nevertheless, as Mather (1999) suggested, either "hard" or "soft" classifications was not an appropriate tool for the analysis of heterogeneous landscapes. Both Ridd (1995) and Mather (1999) maintained that identification/description/quantification, rather than classification, should be applied in order to provide a better understanding of the compositions and processes of heterogeneous landscapes such as urban areas.

Ridd (1995) proposed an interesting conceptual model for remote sensing analysis of urban landscapes, *i.e.*, the vegetation–impervious surface–soil (V–I–S) model. It assumes that land cover in urban environments is a linear combination of three components, namely, vegetation, impervious surface, and soil. Ridd suggested that this model can be applied to spatial–temporal analyses of urban morphology, biophysical, and human systems. While urban land use information may be more useful in socioeconomic and planning applications, biophysical information that can be directly derived from satellite data is more suitable for describing and quantifying urban structures and processes (Ridd, 1995). The V–I–S model was developed for Salt Lake City, Utah, but has been tested in other cities. Ward et al. (2000) applied a hierarchical unsupervised classification approach to a Landsat TM image in southeast Queensland, Australia, based on the V–I–S model. An adjusted overall accuracy of 83% was achieved. Madhavan et al. (2001) used an unsupervised classifier to classify TM images in Bangkok, Thailand, with the V–I–S model, and found it to be useful for improving classification and analysis of change trends. Similarly, Setiawan et al. (2006) applied a V–I–S based hieratical procedure to classify a Landsat TM image of Yogyakarta, Indonesia, and found its accuracy was 27% better than the maximum likelihood algorithm. All of these studies employed the V–I–S model as the conceptual framework to relate urban morphology to medium-resolution satellite imagery, but "hard classification" algorithms were applied. Therefore, the problem of mixed pixels cannot be addressed, and the analysis of urban landscapes was still based on "pixels" or "pixel groups". Weng and Lu (2009) suggested that LSMA provided a suitable technique to detect and map urban materials and V–I–S component surfaces in repetitive and consistent ways, and to solve the spectral mixing of medium spatial resolution imagery. The reconciliation between the V–I–S model and LSMA provided a continuum field model, which offered an alternative, effective approach for characterizing and quantifying the spatial and temporal changes of the urban landscape compositions. However, Weng and Lu (2009) warned

that the applicability of this continuum model must be further examined in terms of its spectral, spatial, and temporal variability.

3.3. Artificial neural network

Artificial Neural Network (ANN) has been widely used in remote sensing image analysis. The most common application is for image classification (Atkinson & Tatnall, 1997). While the majority of previous researches employs ANN as a per-pixel classifier (Chen et al., 1995; Civco, 1993; Foody et al., 1995), ANN has also been applied to estimate sub-pixel impervious surfaces from satellite images (Flanagan & Civco, 2001; Hu & Weng, 2009; Lee & Lathrop, 2006; Mohapatra & Wu, 2007; Weng & Hu, 2008). Advantages of an ANN model include its capability of solving non-linear relationships, no underlying assumption about the data, incorporation of *a priori* knowledge, and the ability to incorporate different types of data into the analysis (Atkinson & Tatnall, 1997). Moreover, ANN requires fewer training samples (Pal & Mather, 2003). Various types of neural networks have been employed for image analysis, including Hopfield Neural Networks, Multi-Layer Perceptron (MLP), ARTMAP, and Self-Organizing Map (SOM), but MLP and SOM are mostly used in remote sensing of impervious surfaces. Table 3 provides a summary of the characteristics, strengths and limitations for these two neural network models, with relevant literature.

The multi-layer perceptron feed forward network is the most widely used one in remote sensing studies (Kavzoglu & Mather, 2003). The learning algorithm is crucial to the success of an ANN model. The back-propagation learning algorithm, also known as delta rule, is a popular one. The MLP has been used in impervious surface extraction (Chormanski et al., 2008; Mohapatra & Wu, 2007; Weng & Hu, 2008). Chormanski et al. (2008) conducted a multi-layer perceptron model to map the fractions of impervious surfaces, vegetation, bare soil, and water/shade with both high spatial resolution and medium resolution imagery. It is suggested that sub-pixel estimation of impervious surface distribution can be used to substitute for the expensive high-resolution based approach for rainfall-runoff modeling. Mohapatra and Wu (2007) used a three-layer feed forward back propagation neural network to estimate the percentage of impervious surfaces by creating activation level maps from high spatial resolution imagery (*i.e.*, IKONOS). Their result indicated that ANN model performed well in the urban areas and was promising for impervious surface estimation from high spatial resolution imagery. Weng and Hu (2008) employed MLP feed forward network with the back-propagation learning algorithm as a sub-pixel image classifier to estimate impervious surfaces in Indianapolis, U.S.A. It is found that the ANN model improved the accuracy of impervious surface mapping by 1% and 2% for ASTER and Landsat ETM+ image respectively. The better performance of ANN over LSMA was mainly attributable to the ANN's capability of handling the non-linear mixing of image spectrum. Fig. 3 shows that the ANN model delineated a much clearer pattern of impervious surfaces than LSMA in a residential area where mixed pixels prevailed. Although MLP has been widely used in remote sensing, some drawbacks should be noted. For instance, how to design the number of hidden layers and the number of hidden layer nodes in the model are challenging issues. Although several methods have been suggested for estimating the appropriate number of hidden layer nodes, none of them are universally accepted (Kavzoglu & Mather, 2003). Another problem of MLP is that MLP requires the training sites to include both presence and absence data. The desired output must contain both true and false information, so that the network can learn all kinds of patterns in a study area in order to classify an image accordingly (Li & Eastman, 2006a). However, in some cases, absence data is not available. Therefore, MLP might not be suitable for those cases, and other ANN models should be explored for use. Finally, MLP has the local minima problem in the training process, which significantly affects the accuracy of the result.

Another neural network approach, Kohonen's self-organizing map (SOM), has not been applied as widely as MLP (Pal et al., 2005). SOM can be used for both supervised and unsupervised classifications, and has the properties for both vector quantization and projection (Li & Eastman, 2006a). SOM has been used for both "hard" classification and "soft" classification in previous studies (Ji, 2000; Lee & Lathrop, 2006). Ji (2000) compared Kohonen self-organizing feature map (KSOFM) and MLP for image classification at per-pixel level. Seven classes were identified, and the result showed that SOM provided an excellent alternative to MLP neural network in "hard" classification. Lee and Lathrop (2006) conducted a SOM–LVQ–GMM to extract urban land cover from Landsat ETM+ imagery at sub-pixel level. It is found that SOM can generate promising results in "soft" classification and that SOM had several advantages over MLP. Hu and Weng (2009) compared MLP with SOM to estimate impervious surfaces at the sub-pixel level of three ASTER images of Marion County, Indiana, USA, and found that SOM outperformed MLP slightly for each season of image data, especially in the residential areas. Comparing to MLP, SOM possesses clearly some strengths. First, SOM is a two-layer structure, including one input layer and one output layer. Therefore, the dilemma of determining the hidden layer size can be avoided. Second, SOM is capable of coping with presence-only data (Li & Eastman, 2006a). Third, the SOM is not affected by the local minima problem in the training process, and is insensitive to the structure of the codebook vector map (Lee & Lathrop, 2006). Fourth, the feature map is a faster learner. Finally, the feature map is also more consistent than the BP algorithm (Ji, 2000). Nevertheless, the classification process of the SOM is slower than the MLP, and the accuracy level is heavily relied on the size of the feature map. Too few or too many neurons may significantly increase the RMSE of the estimation result. Therefore, an appropriate size of the SOM map must be established in order to achieve the best result of impervious surface estimation (Hu & Weng, 2009). In addition, the number of training samples selected for each class also affects the performance of SOM (Ji, 2000). Therefore, the number of samples selected for each class needs to be balanced.

Table 3
Use of artificial neural networks in remote sensing impervious surfaces.

Techniques	Characteristics	Advantages	Disadvantages	Literatures	
Multi-Layer Perceptron (MLP)	Multiple layers structure, usually consists of three layers: one input layer, one hidden layer, and one output layer	Fast computation	Slow learning; inconsistent classification results; black-box working method	Per-pixel Sub-pixel	Civco (1993) Mohapatra & Wu, 2007; Chormanski et al., 2008; Weng & Hu, 2008
Kohonen's Self-Organizing Map (SOM)	Consist of two layers: one input layer and one output layer. The input layer contains neurons for each measurement dimension (*e.g.*, image bands), and the output layer is usually organized as a two-dimension array of neurons.	Fast learning, classification results are more consistent	Slow classification	Per-pixel Sub-pixel	Ji, 2000; Li & Eastman, 2006b Lee & Lathrop, 2006; Hu & Weng, 2009

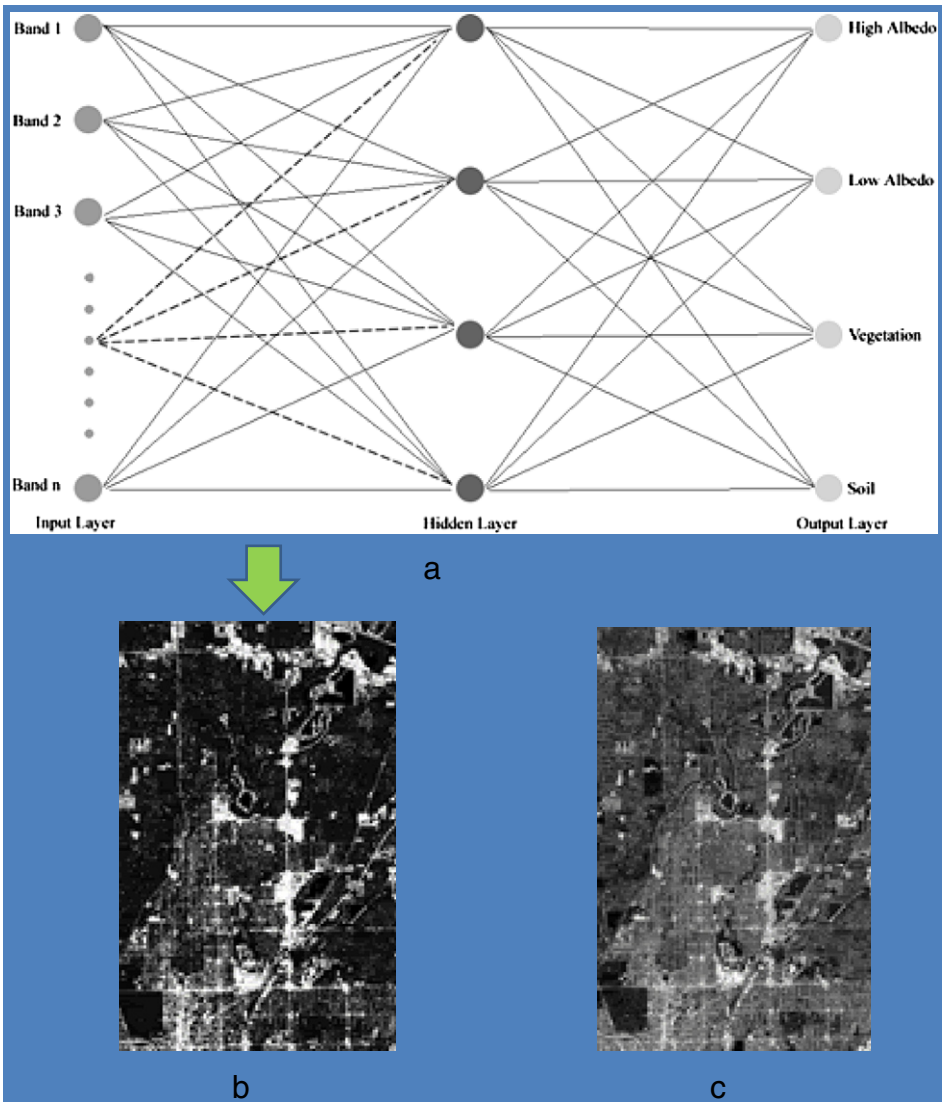

Fig. 3. (a) Illustration of three layer neural network structure used in the study. In the input layer, nine nodes represented nine reflective bands of the ASTER image; while four training surface material classes were selected, *i.e.*, high albedo, low albedo, vegetation and soil. Only one hidden layer was used and the number of hidden layers nodes was four. (b) Impervious surface map generated by the ANN model, with an accuracy of 12.3% for the whole study area. (3) Impervious surface map resulted from linear spectral mixture analysis, with an accuracy of 13.2% for the whole study area.

3.4. Object based image analysis

Object based image analysis (OBIA) has been increasingly used in remote sensing applications due to the advent of high resolution satellite imagery and the emergence of commercial software (Benz et al., 2004; Wang et al., 2004). In previous studies, various image segmentation techniques have been developed and applied for feature extraction with a fair amount of success (Blaschke, 2010). However, most of the segmentation techniques are not robust enough for a spectrally complex environment (Pal & Pal, 1993), which makes them less suitable for urban classification. Therefore, it is necessary to continue to develop new techniques. The OBIA approach uses not only the spectral properties, but also the characteristics of shape, texture, context, and relationship with neighbors, super-, and sub-pixels. Successful results have been obtained by this approach (Van de Voore et al., 2003). In a comparative study, Yuan and Bauer (2006) compared the effectiveness of OBIA with per-pixel maximum likelihood classification for urban classification with a QuickBird image of Mankato, Minnesota. With OBIA, they improved the producer's accuracy by 2% and the user's accuracy by 3% for impervious surfaces. Zhou and Wang (2008) developed an algorithm of multiple agent segmentation and classification (MASC) that included the steps of image segmentation, shadow-effect, MANOVA-based classification, and post-classification. This algorithm was applied for impervious surface extraction in the state of Rhode Island. In addition, rule-based classification is another method to classify image objects. However, traditional rule-based classification is based on strict binary rules. Objects are assigned to a class if the objects are meeting the rules of that class. These rules may not be suitable for classifying objects, because the attributes of different features may overlap (Jin & Paswaters, 2007). Fuzzy logic can better cope with the uncertainties inherent in the data and vagueness in human knowledge (Jin & Paswaters, 2007). Hu and Weng (2011) developed an object-based fuzzy classification approach for impervious surface extraction, which was applied to two pan-sharpened multi-spectral IKONOS images covering the residential and Central Business District (CBD) areas of Indianapolis, U.S.A. Fuzzy rules were developed to extract impervious surfaces based on spectral, spatial, and texture attributes. Their results indicated that impervious surfaces were extracted with an accuracy of 95% in the residential area and 92% in the CBD area. It is suggested that the CBD area had a higher spectral complexity, building displacement, and the shadow problem, giving rise to a more difficult estimation and mapping of impervious surfaces (Hu & Weng, 2011).

In addition, LiDAR data have been applied to quite a few studies in object-oriented classification of urban land use and land cover (LULC). Zhou and Troy (2008) combined aerial imagery and LiDAR data for an object-oriented classification of urban LULC and achieved an overall accuracy of 92.3%. Brennan and Webster (2006) proposed an objected-oriented LULC classification method by solely using LiDAR-derived surfaces, including DSM, DEM, intensity, multiple echoes, and normalized height. In the classification, the average accuracy of ten classes reached 94%, while it can be improved to 98% if aggregated into seven classes. Due to LiDAR data's characteristics in geometry, object-oriented classification techniques have a great potential in extracting buildings and roads in the urban areas. The similarity of urban feature classes (*e.g.*, buildings) in spectral, spatial, and textural information, such as height, shape and texture, enables merging discrete points or pixels into objects of similar properties close to real spatial objects, which can then be interpreted into a high-qualified image based knowledge (Gitas et al., 2004). Miliaresis and Kokkas (2007) developed an object-oriented method to extract buildings by using LiDAR DEM, which was based on seed cells and region growing criteria. However, this method required a certain level of user interface for crucial parameters and was time-consuming. Weng (2009) used LiDAR data (specifically, normalized height model) to extract buildings for the downtown Indianapolis. Three building extraction strategies were adopted and compared, including rule-based extraction with segmentation, rule-based extraction with segmentation and merge, and supervised object-oriented extraction, and yielded an accuracy of extraction (detection percentage) of 88.5%, 80% and 93.4% respectively. It was found that extraction errors were mainly caused by trees mislabeled as buildings, and by buildings mislabeled as background (Fig. 4). Similarly, Yu et al. (2010) extracted buildings in the downtown Houston, and computed building density indicators at land lot and urban district scales.

4. Discussion on emerging methods

4.1. Data and image fusion

Data and image fusion can be implemented between different sensors, wavelength regions, spatial, spectral, and temporal resolutions. Images from different sensors contain distinctive features. Data fusion or integration of multi-sensor or multi-resolution data takes advantage of the strengths of distinct image data for improvement of visual interpretation and quantitative analysis. In general, three levels of data fusion may be identified, *i.e.*, pixel (Luo & Kay, 1989), feature (Jimenez et al., 1999), and decision (Benediktsson & Kanellopoulos, 1999). Many methods have been developed to fuse spectral and spatial information in previous literature (Chen & Stow, 2003; Gong, 1994; Lu & Weng, 2005; Pohl & Van Genderen, 1998). Solberg et al. (1996) broadly divided data fusion methods into four categories: statistical, fuzzy logic, evidential reasoning, and neural network. Pohl and Van Genderen (1998) provided a literature review on the methods of multisensor data fusion. The methods, including color-related techniques (*e.g.*, color composite, intensity–hue–saturation or IHS, and luminance–chrominance), statistical/mathematical methods (*e.g.*, arithmetic combination, principal component analysis, high pass filtering, regression variable substitution, canonical variable substitution, component substitution, and wavelets), and various combinations

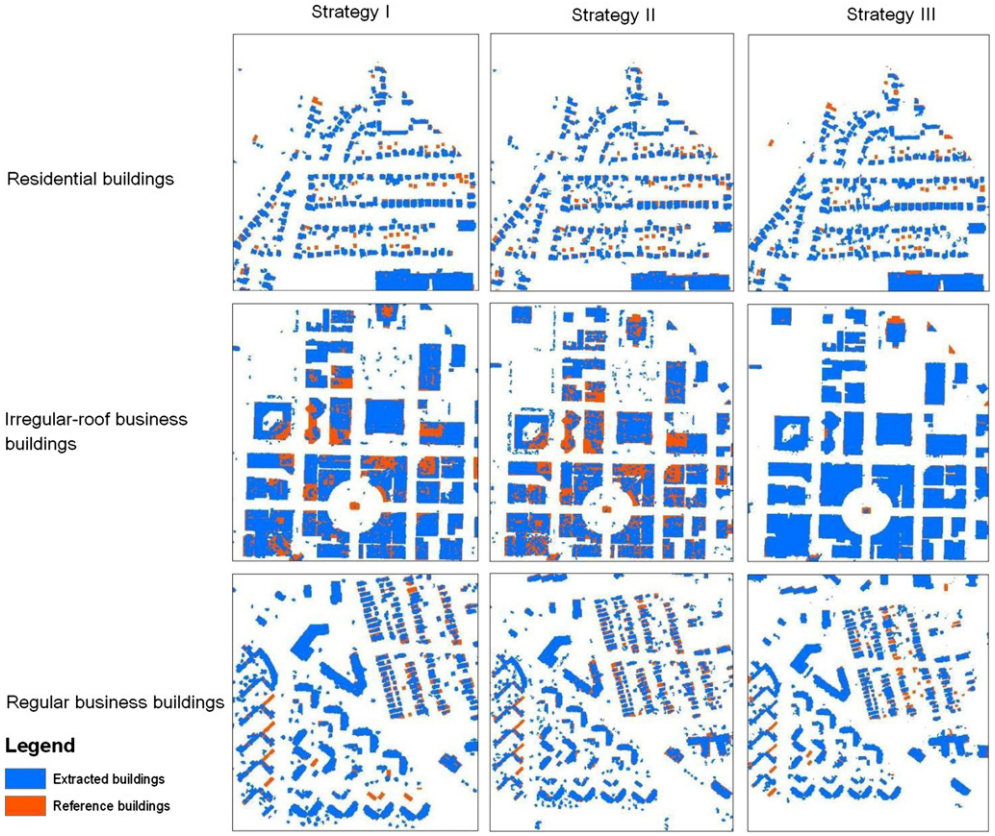

Fig. 4. LiDAR data acquired in March and April 2003 was used to extract buildings in the downtown Indianapolis, U.S.A. Errors due to mislabeled building pixels. Supervised object-oriented extraction method (Strategy III) had the least amount of building pixels lost during the extraction, thus possessed the highest accuracy. The amount of extracted residential buildings and regular business buildings were similar with Strategy I (rule-based extraction with segmentation) and Strategy II (rule-based extraction with segmentation and merge). Missed pixels of irregular-roof business buildings accounted for the majority of errors in both Strategies I and II. Large variation in height of the irregular roofs can easily lead to over-segmentation and produced large amount of fragmented small objects, which may be eliminated in the process of building extraction. In addition, Strategy II had the largest amount of missed pixels of irregular-roof business buildings, because the *Merge* operation combined fragmented small objects into larger objects, which were frequently not large enough to be kept, leading to missing of more pixels.

of the above methods, have been studied. Previous research indicated that integration of optical data, such as Landsat TM imagery, and radar (Ban, 2003; Haack et al., 2002) can improve image classification results. Yang et al. (2009) integrated four SPOT HRG multispectral bands and three Interferometric SAR parameters (*i.e.*, coherence, average amplitude, and amplitude ratio) to estimate impervious surface at the sub-pixel level in Hong Kong using the CART algorithm. It is found that the estimation error reduced from 15.5% (optical data alone) to 12.9% (the combined dataset), and the improvement was especially helpful in separation of the urban impervious surface from vacant land or bare ground. Lu and Weng (2006) employed Landsat thermal infrared (TIR) data to remove pervious cover from impervious cover based on their distinct thermal response. They found that the method was effective for reducing the underestimation in well-developed areas and the overestimation in the less-developed areas, and the overall RMSE of 9.22% was achieved for the whole Marion County, Indiana, United States. Weng et al. (2009) applied LSMA to estimate impervious surfaces in Indianapolis from ASTER images of different seasons, and found that using land surface temperature maps of water and vegetation as image masks can significantly improve the accuracy of estimation. The most remarkable improved was observed in the April image (9%), followed by the October image (7%) and June image (3%). Because there was significant amount of bare soil and ground and non-photosynthetic vegetation in the spring and autumn images, LSMA was less effective. Thus, the use of TIR data was instrumental in producing impervious surfaces maps of reasonable accuracy.

4.2. Knowledge based expert systems

Expert systems are considered to have a great potential for providing a general approach to the routine use of image ancillary data in image classification (Hinton, 1996). A critical step is to develop rules that can be applied in an expert system or a knowledge based classification approach. According to Hodgson et al. (2003), three methods have been employed to build rules for image classification, *i.e.*, (1) explicitly eliciting knowledge and rules from experts and then refining the rules (Hung & Ridd, 2002; Stefanov et al., 2001; Stow et al., 2003), (2) implicitly extracting variables and rules using cognitive methods (Hodgson, 1998; Lloyd et al., 2002), and (3) empirically generating rules from observed data with automatic induction methods (Hodgson et al., 2003; Huang & Jensen, 1997; Tullis & Jensen, 2003). Among these methods, the automatic induction has generated increasing interest because of relatively low effort and reasonable performance (Hodgson et al., 2003). The approach of knowledge based expert systems is especially attractive where the combined use of multiple sources of data such as satellite imagery and GIS data are necessary. GIS plays an important role in developing and implementing knowledge based classification approaches, because of its capability in integrating different sources of data and in spatial modeling (Lu & Weng, 2007). Hodgson et al. (2003) employed a rule-based classifier (a rule-generation package, See 5) to map urban parcel impervious surface, and found it to be effective at both pixel and segment levels. The rule-based segment classifier produced the best result among all methods being compared, and was nearly perfect in predicting imperviousness for the parcels with low imperviousness. Lu and Weng (2006) developed two rules by using Landsat TIR data and abundance of soil fraction for refining the impervious surface map derived from LSMA, and found the method was effective, especially in the highly urbanized and under-developed areas. Powell et al. (2008) devised a set of knowledge-based rules for refining LSMA based classification results so that change detection can be made. Two spatial rules were applied independently to each date of the images in the time series for subdividing the low vegetation and no vegetation classes into impervious and non-impervious classes; while two temporal rules were devised to rectify some incongruous pixel-level temporal trajectories of class labels that resulted from the use of the spatial rules. Powell et al. (2008) suggested that their rules can effectively distinguish impervious surfaces from open, non-vegetated surfaces, which were spectrally indistinguishable. Similarly, the population, housing and road-density data may be incorporated into an urban classification procedure with different ways to improve classification accuracy. Population-, housing-, and road-densities are related to urban land use distribution, and may be very helpful in the distinctions between commercial/industrial lands and high intensity residential lands, between recreational grassland and pasture/crops, or the distinction between residential areas and forest land (Lu & Weng, 2006). Li (2008) developed seven rules based on housing density to refine Landsat ETM+ derived urban LULC classification result in Indianapolis. It is found that the post-classification sorting enhanced most the accuracy of residential land, and that the overall classification accuracy improved by 8.5%.

4.3. Contextual classifications

Contextual classifications exploit spatial information among neighboring pixels to improve classification performance (Flygare, 1997; Stuckens et al., 2000). Contextual classifiers may base on smoothing techniques, Markov random fields, spatial statistics, fuzzy logic, segmentation, or neural network (Binaghi et al., 1997; Cortijo & de la Blanca, 1998; Kartikeyan et al., 1994; Magnussen et al., 2004). In general, pre-smoothing classifiers incorporates contextual information as additional bands, and a classification is then conducted using normal spectral classifiers, while post-smoothing classifiers is conducted on classified images that are developed previously using spectral based classifiers (Lu & Weng, 2007). The Markov random field based contextual classifiers such as iterated conditional modes are the most frequently used approach in contextual classification (Cortijo & de la Blanca, 1998; Magnussen et al., 2004), and has proven effective in improving classification results. Contextual classifiers may be developed to cope with the problem of intra-class spectral variations (Flygare, 1997; Gong & Howarth, 1992; Kartikeyan et al., 1994; Keuchel et al., 2003; Magnussen et al., 2004; Sharma & Sarkar, 1998). In remote sensing of impervious surfaces, the use of contextual information serves to improve the separability between impervious surfaces and the most confusing LULC types (*e.g.* dry soils, non-photosynthesis vegetation, and open ground with little vegetation). Powell et al., 2008 developed refinement rules based on spatial context of impervious surfaces, specifically the relationship between impervious surfaces and little or no vegetation cover. Weng et al. (2009) developed image masks based on selected LULC types or their combination. They found that the water–forest mask was most effective in improving the impervious surface mapping results for the October and April ASTER images, but the water–cropland mask the best fit for the June image. Apparently, impervious surface calculated from LSMA had much influence from low albedo materials including water and shade, and it was also confused with fallow lands and non-photosynthesis vegetation in the fall and spring. In addition, Luo and Mountrakis (2010) used intermediate inputs from partially classified images to enhance the spectral separability impervious surfaces and soils. The additional intermediate inputs were based on spatial and texture statistics, and the method was experimented using a 2001 Landsat ETM+ image from central New York. Their results suggested that there was an average accuracy improvement of 3.6% in the final impervious surface map by using these intermediate inputs.

5. Conclusions

Existing remote sensing literature has regarded impervious surface as a type of surface material, land cover, or land use. The discrepancy in conceptual view has stimulated research into three major directions. Various sub-pixel algorithms applied largely to medium-resolution but less frequently to high-resolution imagery to estimate and mapping impervious surfaces as a type of surface material. Per-pixel algorithms were employed for all sorts of images at various spatial resolutions to

classify impervious surfaces as a type of land cover or land use. Feature extraction methods were applied mainly to high resolution satellite imagery, aerial photographs, and LiDAR data to extract roads and buildings, implicitly suggesting impervious surface as a special type of land use/cover. These research directions are sometime intermingled in a study, but clearly they represent different research traditions and have been approached from different perspectives. While feature extraction has long been a favorite research concentration in Europe and to less extent in Asia, the North America researchers have paid more attention to mapping impervious surfaces as a special type of land cover or land use.

Many research endeavors have been oriented towards the spatial heterogeneity of urban landscapes, ideal spatial resolution for urban mapping, and the strengths and limitations of existing remote sensors. In contrast, less research efforts have been devoted to the spectral diversity of impervious surfaces and the spectral requirements for remote sensing of impervious surfaces. Hyperspectral imaging has been applied most extensively in the studies of vegetation and water but little to impervious surfaces. Similarly, the geometric properties (especially the 3-D nature) of urban environments have been under-studied. Digital orthophotos have become widely available statewide or nationwide, suitable for monitoring and assessing surface cover conditions, but stereo-pairs of photographs were acquired only for limited areas, largely for measurements, not for mapping urban impervious surfaces. The enthusiasm over LiDAR data has prompted some interest in extraction of buildings but to less degree roads. The least attention was paid to temporal resolution, change and evolution of impervious surface over time, and temporal requirements for urban mapping. Therefore, there is a great need to address the temporal resolution requirements in urban remote sensing and how it relates to spectral resolution, spatial resolution, and the geometric characteristics of urban features and objects. Of course, we have to link these research traits to the capacities of various remote sensors, sensing systems and platforms over the time. It is pleased to learn that the Decadal Survey (National Research Council, 2007) has suggested improving the temporal resolution of satellites capable of urban imaging (*e.g.*, HyspIRI sensor). The MISTIGRI project, a satellite designed to observe the Earth in the thermal infrared region, which has been proposed to be developed by the French space organization CNES in cooperation with Spain (Laguarde et al., 2010), shows a similar interest in "high-definition" urban remote sensing.

The majority of previous remote sensing studies of impervious surfaces have used medium spatial resolution images. The models, methods, and image analysis algorithms in urban remote sensing have been geared largely towards the images of such resolution. The advent of high spatial resolution satellite images, spaceborne hyperspectral images and LiDAR data has provided an unprecedented opportunity for urban remote sensing, and at the meantime, is challenging the traditional remote sensing concepts, models, and image processing algorithms. The temptation to take advantage of the opportunity to combine ever-increasing computational power, more plentiful and capable digital data, and more advanced algorithms has driven the field of urban remote sensing into a new frontier of scientific inquiry. The following emerging trends in image processing techniques and data analysis methods will advance remote sensing of impervious surfaces in the future. These trends include: (1) attribute analysis and information extraction by more powerful ANN models and knowledge-based expert systems, (2) object-based image analysis, and (3) enhanced urban mapping via data and image fusion of different sensors, wavelength regions, spatial, spectral, and temporal resolutions. In addition, we have witnessed an increasing number of studies that explore the combined use of contextual, texture, and spatial information with the spectral characteristics of impervious surfaces.

Acknowledgments

The author wishes to thank Drs. Xuefei Hu, Dengsheng Lu, and Mrs. Jing Han for their assistance in research, which contributes to this review. Dr. Marvin Bauer kindly provides editing and valuable comments for improving the manuscript. The author would also like to thank anonymous reviewer for the constructive comments and suggestions.

References

Adams, J. B., Smith, M. O., & Johnson, P. E. (1986). Spectral mixture modeling: A new analysis of road and soil types at the Viking Lander site. *Journal of Geophysical Research*, *91*, 8098–8112.

Amini, J., Saradjian, M. R., Blais, J. A. R., & Azizi, A. (2002). Automatic road-side extraction from large scale image maps. *International Journal of Applied Earth Observation and Geoinformation*, *4*(2), 96–98.

Arnold, C. L., Jr., & Gibbons, C. J. (1996). Impervious surface coverage: The emergence of a key environmental indicator. *Journal of the American Planning Association*, *62*, 243–258.

Atkinson, P. M., & Tatnall, A. R. L. (1997). Neural networks in remote sensing. *International Journal of Remote Sensing*, *18*, 699–709.

Bagheri, S., & Yu, T. (2008). Hyperspectral sensing for assessing nearshore water quality conditions of Hudson/Raritan estuary. *Journal of Environmental Informatics*, *11*(2), 123–130.

Ban, Y. (2003). Synergy of multitemporal ERS-1 SAR and Landsat TM data for classification of agricultural crops. *Canadian Journal of Remote Sensing*, *29*, 518–526.

Bauer, M. E., Heinert, N. J., Doyle, J. K., & Yuan, F. (2004). Impervious surface mapping and change monitoring using Landsat remote sensing. *ASPRS Annual Conference Proceedings, Denver, Colorado, May 2004* (Unpaginated CD ROM).

Bauer, M. E., Loffelholz, B. C., & Wilson, B. (2007). Estimating and mapping impervious surface area by regression analysis of Landsat imagery. In Q. Weng (Ed.), *Remote sensing of impervious surfaces* (pp. 3–19). Boca Raton, Florida: CRC Press.

Ben-Dor, E., Levin, N., & Saaroni, H. (2001). A spectral based recognition of the urban environment using the visible and near-infrared spectral region (0.4–1.1 m) — A case study over Tel-Aviv. *International Journal of Remote Sensing*, *22*(11), 2193–2218.

Benediktsson, J. A., & Kanellopoulos, I. (1999). Classification of multisource and hyperspectral data based on decision fusion. *IEEE Transactions on Geoscience and Remote Sensing*, *37*, 1367–1377.

Benediktsson, J. A., Sveinsson, J. R., & Arnason, K. (1995). Classification and feature extraction of AVIRIS data. *IEEE Transactions on Geoscience and Remote Sensing*, *33*, 1194–1205.

Benz, U. C., Hofmann, P., Willhauck, G., Lingenfelder, I., & Heynen, M. (2004). Multi-resolution, object-oriented fuzzy analysis of remote sensing data for GIS-ready information. *ISPRS Journal of Photogrammetry and Remote Sensing*, *58*, 239–258.

Binaghi, E., Madella, P., Montesano, M. G., & Rampini, A. (1997). Fuzzy contextual classification of multisource remote sensing images. *IEEE Transactions on Geoscience and Remote Sensing*, *35*, 326–339.

Blaschke, T. (2010). Object based image analysis for remote sensing. *ISPRS Journal of Photogrammetry and Remote Sensing*, *65*, 2–16.

Bloch, I. (1996). Information combination operators for data fusion: a comparative review with classification. *IEEE Transactions on Systems, Man, and Cybernetics*, *26*, 52–67.

Boardman, J. W. (1993). Automated spectral unmixing of AVIRIS data using convex geometry concepts. *Summaries of the Fourth JPL Airborne Geoscience Workshop, JPL Publication 93–26* (pp. 11–14). Pasadena, California: NASA Jet Propulsion Laboratory.

Boardman, J. M., Kruse, F. A., & Green, R. O. (1995). Mapping target signature via partial unmixing of AVIRIS data. *Summaries of the Fifth JPL Airborne Earth Science Workshop, JPL Publication 95–1* (pp. 23–26). Pasadena, California: NASA Jet Propulsion Laboratory.

Boegh, E., Poulsen, R. N., Butts, M., Abrahamsen, P., Dellwik, E., Hansen, S., et al. (2009). Remote sensing based evapotranspiration and runoff modeling of agricultural, forest and urban flux sites in Denmark: From field to macro-scale. *Journal of Hydrology*, *377*(3–4), 300–316.

Brabec, E., Schulte, S., & Richards, P. L. (2002). Impervious surface and water quality: A review of current literature and its implications for watershed planning. *Journal of Planning Literature*, *16*, 499–514.

Braun, C., Kolbe, T. H., Lang, F., Schickler, W., Cremers, A. B., Forstner, W., et al. (1995). Models for photogrammetric building reconstruction. *Computer and Graphics*, *19*(1), 109–118.

Brennan, R., & Webster, T. L. (2006). Object-oriented land cover classification of LiDAR-derived surfaces. *Canadian Journal of Remote Sensing*, *32*(2), 162–172.

Brun, S. E., & Band, L. E. (2000). Simulating runoff behavior in an urbanizing watershed. *Computers, Environment and Urban Systems*, *24*, 5–22.

Cablk, M. E., & Minor, T. B. (2003). Detecting and discriminating impervious cover with high resolution IKONOS data using principal component analysis and morphological operators. *International Journal of Remote Sensing*, *24*, 4627–4645.

Carlson, T. N. (2004). Analysis and prediction of surface runoff in an urbanizing watershed using satellite imagery. *Journal of the American Water Resources Association*, *40*(4), 1087–1098.

Carlson, T. N., & Arthur, S. T. (2000). The impact of land use–land cover changes due to urbanization on surface microclimate and hydrology: A satellite perspective. *Global and Planetary Change*, *25*, 49–65.

Carlson, T. N., & Ripley, A. J. (1997). On the relationship between fractional vegetation cover, leaf area index and NDVI. *Remote Sensing of Environment*, *62*, 241–252.

Chabaeva, A. A., Civco, D. L., & Prisloe, S. (2004). Development of a population density and land use based regression model to calculate the amount of imperviousness. *ASPRS Annual Conference Proceedings, Denver, Colorado, May 2004* (Unpaginated CD ROM).

Chen, D., & Stow, D. A. (2003). Strategies for integrating information from multiple spatial resolutions into land-use/land-cover classification routines. *Photogrammetric Engineering and Remote Sensing*, *69*, 1279–1287.

Chen, K. S., Tzeng, Y. C., Chen, C. F., & Kao, W. L. (1995). Land-cover classification of multispectral imagery using a dynamic learning neural network. *Photogrammetric Engineering and Remote Sensing*, *61*(4), 403–408.

Chormanski, J., Voorde, T. V. d., Roeck, T. D., Batelaan, O., & Canters, F. (2008). Improving distributed runoff prediction in urbanized catchments with remote sensing based estimates of impervious surface cover. *Sensors*, *8*, 910–932.

Civco, D. L. (1993). Artificial neural networks for land-cover classification and mapping. *International Journal of Geographical Information Systems*, *7*(2), 173–186.

Civco, D. L., Hurd, J. D., Wilson, E. H., Arnold, C. L., & Prisloe, M. P., Jr. (2002). Quantifying and describing urbanizing landscapes in the northeast United States. *Photogrammetric Engineering and Remote Sensing*, *68*(10), 1083–1090.

Clode, S., Kootsookos, P., & Rottensteiner, F. (2004). The automatic extraction of roads from LIDAR data. *International Archives of Photogrammetry, Remote Sensing and Spatial Information Science*, *Vol. XXXV-B3*, 231–236.

Clode, S., Kootsookos, P., & Rottensteiner, F. (2005). Improving city model determination by using road detection from Lidar data. In U. Stilla, F. Rottensteiner, & S. Hinz (Eds.), *CMRT05. IAPRS, Vol. XXXVI, Part 3/W24* (pp. 159–164). Vienna, Austria, August 29–30, 2005.

Clode, S., Rottensteinerb, F., Kootsookosc, P., & Zelniker, E. (2007). Detection and vectorization of roads from LiDAR data. *Photogrammetric Engineering and Remote Sensing*, *73*(5), 517–535.

Cortijo, F. J., & de la Blanca, N. P. (1998). Improving classical contextual classification. *International Journal of Remote Sensing*, *19*, 1591–1613.

Cracknell, A. P. (1998). Synergy in remote sensing — What's in a pixel? *International Journal of Remote Sensing*, *19*, 2025–2047.

Cracknell, A. P. (1999). Twenty years of publication of the *International Journal of Remote Sensing*. *International Journal of Remote Sensing*, *20*, 3469–3484.

Cushnie, J. L. (1987). The interactive effect of spatial resolution and degree of internal variability within land-cover types on classification accuracies. *International Journal of Remote Sensing*, *8*, 15–29.

Dare, P. M. (2005). Shadow analysis in high-resolution satellite imagery of urban areas. *Photogrammetric Engineering and Remote Sensing*, *71*, 169–177.

DeFries, R. S., & Chan, J. C. (2000). Multiple criteria for evaluating machine learning algorithms for land cover classification from satellite data. *Remote Sensing of Environment*, *74*, 503–515.

Dougherty, M., Dymond, R. L., Goetz, S. J., Jantz, C. A., & Goulet, N. (2004). Evaluation of impervious surface estimates in a rapidly urbanizing watershed. *Photogrammetric Engineering and Remote Sensing*, *70*, 1275–1284.

Elberink, S. O., & Vosselman, G. (2009). 3D information extraction from laser point clouds covering complex road junctions. *The Photogrammetric Record*, *24*(125), 23–36.

Elmore, A. J., & Guinn, S. M. (2010). Synergistic use of Landsat Multispectral Scanner with GIRAS land-cover data to retrieve impervious surface area for the Potomac River Basin in 1975. *Remote Sensing of Environment*, *114*, 2384–2391.

Elvidge, C., Tuttle, B. T., Sutton, P. C., Baugh, K. E., Howard, A. T., Milesi, C., et al. (2007). Global distribution and density of constructed impervious surfaces. *Sensors*, *7*, 1962–1979.

Epstein, J., Payne, K., & Kramer, E. (2002). Techniques for mapping suburban sprawl. *Photogrammetric Engineering and Remote Sensing*, *68*, 913–918.

Filin, S. (2004). Surface classification from airborne laser scanning data. *Computers and Geosciences*, *30*(9–10), 1033–1041.

Fisher, P. (1997). The pixel: A snare and a delusion. *International Journal of Remote Sensing*, *18*, 679–685.

Flanagan, M., & Civco, D. L. (2001). Subpixel impervious surface mapping. *ASPRS Annual Conference Proceedings, St. Louis, Missouri, April 2001* (Unpaginated CD ROM).

Flygare, A. -M. (1997). A comparison of contextual classification methods using Landsat TM. *International Journal of Remote Sensing*, *18*, 3835–3842.

Foody, G. M. (1999). Image classification with a neural network: from completely-crisp to fully-fuzzy situation. In P. M. Atkinson, & N. J. Tate (Eds.), *Advances in Remote Sensing and GIS Analysis* (pp. 17–37). New York: John Wiley and Sons.

Foody, G. M., & Arora, M. K. (1997). An evaluation of some factors affecting the accuracy of classification by an artificial neural network. *International Journal of Remote Sensing*, *18*, 799–810.

Foody, G. M., Lucas, R. M., Curran, P. J., & Honzak, M. (1997). Non-linear mixture modelling without end-members using an artificial neural network. *International Journal of Remote Sensing*, *18*, 937–953.

Foody, G. M., McCulloch, M. B., & Yates, W. B. (1995). Classification of remotely sensed data by an artificial neural network: Issues related to training data characteristics. *Photogrammetric Engineering and Remote Sensing*, *61*, 391–401.

Forlani, G., Nardinocchi, C., Scaioni, M., & Zingaretti, P. (2006). Complete classification of raw LIDAR data and 3D reconstruction of buildings. *Pattern Analysis and Applications*, *8*(4), 357–374.

Franke, J., Roberts, D. A., Halligan, K., & Menz, G. (2009). Hierarchical Multiple Endmember Spectral Mixture Analysis (MESMA) of hyperspectral imagery for urban environments. *Remote Sensing of Environment*, *113*, 1712–1723.

Gamba, P., & Herold, M. (2009). *Global mapping of human settlements: Experiences, datasets, and prospects.* Boca Raton, FL: CRC Press.

Gillies, R. R., Box, J. B., Symanzik, J., & Rodemaker, E. J. (2003). Effects of urbanization on the aquatic fauna of the Line Creek watershed, Atlanta — A satellite perspective. *Remote Sensing of Environment*, *86*, 411–422.

Gillies, R. R., Carlson, T. N., Cui, J., Kustas, W. P., & Humes, K. S. (1997). A verification of the 'triangle' method for obtaining surface soil water content and energy fluxes from remote measurements of the normalized difference vegetation index (NDVI) and surface temperature. *International Journal of Remote Sensing*, *18*, 3145–3166.

Gitas, I. Z., Mitri, G. H., & Ventura, G. (2004). Object-based image classification for burned area mapping of Creus Cape Spain, using NOAA-AVHRR imagery. *Remote Sensing of Environment*, *92*, 409–413.

Goetz, S. J., Wright, R. K., Smith, A. J., Zinecker, E., & Schaub, E. (2003). IKONOS imagery for resource management: Tree cover, impervious surfaces, and riparian buffer analyses in the mid-Atlantic region. *Remote Sensing of Environment*, *88*, 195–208.

Gong, P. (1994). Integrated analysis of spatial data from multiple sources: An overview. *Canadian Journal of Remote Sensing*, *20*, 349–359.

Gong, P., & Howarth, P. J. (1990). The use of structure information for improving land-cover classification accuracies at the rural–urban fringe. *Photogrammetric Engineering and Remote Sensing*, *56*(1), 67–73.

Gong, P., & Howarth, P. J. (1992). Frequency-based contextual classification and gray-level vector reduction for land-use identification. *Photogrammetric Engineering and Remote Sensing*, *58*(4), 423–437.

Haack, B. N., Solomon, E. K., Bechdol, M. A., & Herold, N. D. (2002). Radar and optical data comparison/integration for urban delineation: A case study. *Photogrammetric Engineering and Remote Sensing*, *68*, 1289–1296.

Heiden, U., Segl, K., Roessner, S., & Kaufmann, H. (2007). Determination of robust spectral features for identification of urban surface materials in hyperspectral remote sensing data. *Remote Sensing of Environment*, *111*, 537–552.

Henricsson, O. (1998). The role of color attributes and similarity grouping in 3-D building reconstruction. *Computer Vision and Image Understanding*, *72*(2), 163–184.

Hepner, G. F., Houshmand, B., Kulikov, I., & Bryant, N. (1998). Investigation of the integration of AVIRIS and IFSAR for urban analysis. *Photogrammetric Engineering and Remote Sensing*, *64*(8), 813–820.

Herold, M. (2007). Spectral characteristics of asphalt road surfaces. In Q. Weng (Ed.), *Remote Sensing of Impervious Surfaces* (pp. 237–247). Boca Raton, Florida: CRC Press.

Herold, M., Liu, X., & Clark, K. C. (2003). Spatial metrics and image texture for mapping urban land use. *Photogrammetric Engineering and Remote Sensing*, *69*(9), 991–1001.

Herold, M., Schiefer, S., Hostert, P., & Roberts, D. A. (2006). Applying imaging spectrometry in urban areas. In Q. Weng, & D. Quattrochi (Eds.), *Urban Remote Sensing* (pp. 137–161). Boca Raton, FL: CRC Press.

Hinton, J. C. (1996). GIS and remote sensing integration for environmental applications. *International Journal of Geographic Information Systems*, *10*(7), 877–890.

Hodgson, M. E. (1998). What size window for image classification? — A cognitive perspective. *Photogrammetric Engineering and Remote Sensing*, *64*, 797–808.

Hodgson, M. E., Jensen, J. R., Tullis, J. A., Riordan, K. D., & Archer, C. M. (2003). Synergistic use of Lidar and color aerial photography for mapping urban parcel imperviousness. *Photogrammetric Engineering and Remote Sensing*, *69*, 973–980.

Hoffbeck, J. P., & Landgrebe, D. A. (1996). Classification of remote sensing having high spectral resolution images. *Remote Sensing of Environment*, *57*, 119–126.

Hsieh, P. -F., Lee, L. C., & Chen, N. -Y. (2001). Effect of spatial resolution on classification errors of pure and mixed pixels in remote sensing. *IEEE Transactions on Geoscience and Remote Sensing*, *39*, 2657–2663.

Hu, J., Razdan, A., Femiani, J., Cui, M., & Wonka, P. (2007). Road network extraction and intersection detection from aerial images by tracking road footprints. *IEEE Transactions on Geoscience and Remote Sensing*, *45*(12), 4144–4157.

Hu, X., & Weng, Q. (2009). Estimating impervious surfaces from medium spatial resolution imagery using the self-organizing map and multi-layer perceptron neural networks. *Remote Sensing of Environment*, *113*(10), 2089–2102.

Hu, X., & Weng, Q. (2011). Impervious surface area extraction from IKONOS imagery using an object-based fuzzy method. *Geocarto International*, *26*(1), 3–20.

Huang, X., & Jensen, J. R. (1997). A machine-learning approach to automated knowledge-base building for remote sensing image analysis with GIS data. *Photogrammetric Engineering and Remote Sensing*, *63*, 1185–1194.

Hung, M., & Ridd, M. K. (2002). A subpixel classifier for urban land-cover mapping based on a maximum-likelihood approach and expert system rules. *Photogrammetric Engineering and Remote Sensing*, *68*, 1173–1180.

Hurd, J. D., & Civco, D. L. (2004). Temporal characterization of impervious surfaces for the State of Connecticut. *ASPRS Annual Conference Proceedings, Denver, Colorado, May 2004* (Unpaginated CD ROM).

Irons, J. R., Markham, B. L., Nelson, R. F., Toll, D. L., Williams, D. L., Latty, R. S., et al. (1985). The effects of spatial resolution on the classification of Thematic Mapper data. *International Journal of Remote Sensing*, *6*, 1385–1403.

Jennings, D. B., Jarnagin, S. T., & Ebert, C. W. (2004). A modeling approach for estimating watershed impervious surface area from national land cover data 92. *Photogrammetric Engineering and Remote Sensing*, *70*, 1295–1307.

Jensen, J. R. (2005). *Introductory digital image processing: A remote sensing perspective* (Third Edition). Upper Saddle River, NJ: Prentice Hall.

Jensen, J. R., & Cowen, D. C. (1999). Remote sensing of urban/suburban infrastructure and socioeconomic attributes. *Photogrammetric Engineering and Remote Sensing*, *65*, 611–622.

Ji, C. Y. (2000). Land-use classification of remotely sensed data using Kohonen self-organizing feature map neural networks. *Photogrammetric Engineering and Remote Sensing*, *66*, 1451–1460.

Jimenez, L. O., Morales-Morell, A., & Creus, A. (1999). Classification of hyperdimensional data based on feature and decision fusion approaches using projection pursuit, majority voting, and neural networks. *IEEE Transactions on Geoscience and Remote Sensing*, *37*, 1360–1366.

Jin, X., & Davis, C. H. (2005). Automated building extraction from high-resolution satellite imagery in urban areas using structural, contextual, and spectral information. *EURASIP Journal on Applied Signal Processing*, *14*, 2196–2206.

Jin, X., & Paswaters, S. (2007). A fuzzy rule base system for object-based feature extraction and classification. In K. Ivan (Ed.), *SPIE* (pp. 65671H).

Kartikeyan, B., Gopalakrishna, B., Kalubarme, M. H., & Majumder, K. L. (1994). Contextual techniques for classification of high and low resolution remote sensing data. *International Journal of Remote Sensing*, *15*, 1037–1051.

Kavzoglu, T., & Mather, P. M. (2003). The use of backpropagating artificial neural networks in land cover classification. *International Journal of Remote Sensing*, *24*, 4907–4938.

Keuchel, J., Naumann, S., Heiler, M., & Siegmund, A. (2003). Automatic land cover analysis for Tenerife by supervised classification using remotely sensed data. *Remote Sensing of Environment*, *86*, 530–541.

Kim, H., Pang, S., Je, H., Kim, D., & Bang, S. Y. (2003). Constructing support vector machine ensemble. *Pattern Recognition*, *36*, 2757–2767.

Laguarde, J. -P., Bach, M., Boulet, G., Briottet, X., Cherchali, S., Dadou, I., et al. (2010). Combining high spatial resolution and revisit capabilities in the thermal infrared: The MISTIGRI Mission Project. In R. Reuter (Ed.), *Proceeding of 30th EARSeL Symposium: Remote Sensing for Science, Education, and Natural and Cultural Heritage* (pp. 165–172). Paris, France: UNESCO May 31–June 3, 2010.

Lang, F., & Forstner, W. (1996). Surface reconstruction of man-made objects using polymorphic mid-level features and generic scene knowledge. *International Archives of Photogrammetry and Remote Sensing*, *31*(B/3), 415–420.

Lawrence, R., Bunn, A., Powell, S., & Zmabon, M. (2004). Classification of remotely sensed imagery using stochastic gradient boosting as a refinement of classification tree analysis. *Remote Sensing of Environment*, *90*, 331–336.

Lee, S., & Lathrop, R. G. (2006). Subpixel analysis of Landsat ETM+ using Self-Organizing Map (SOM) neural networks for urban land cover characterization. *IEEE Transactions on Geoscience and Remote Sensing*, *44*(6), 1642–1654.

Lee, D. H., Lee, K. M., & Lee, S. U. (2008). Fusion of lidar and imagery for reliable building extraction. *Photogrammetric Engineering and Remote Sensing*, *74*(2), 215–225.

Li, G. (2008). Integration of Remote Sensing and Census Data for Land Use and Land Cover Classification and Population Estimation in Indianapolis, Indiana, Ph.D. Dissertation, Department of Geography, Geology, and Anthropology, Indiana State University, Terre haute, Indiana.

Li, Z., & Eastman, J. R. (2006a). *Commitment and typicality measurements for the self-organizing map*. Bellingham, WA: Proceedings of SPIE — The International Society for Optical Engineering (pp. 64201I-1-64201I-4).

Li, Z., & Eastman, J. R. (2006b). The nature and classification of unlabelled neurons in the use of Kohonen's self-organizing map for supervised classification. *Transactions in GIS*, *10*(4), 599.

Lillesand, T. M., Kiefer, R. W., & Chipman, J. W. (2004). *Remote sensing and image interpretation* (pp. 614). New York: John Wiley and Sons.

Linden, S. van der, & Hostert, P. (2009). The influence of urban structures on impervious surface maps from airborne hyperspectral data. *Remote Sensing of Environment*, *113*, 2298–2305.

Lloyd, R. E., Hodgson, M. E., & Stokes, A. (2002). Visual categorization with aerial photography. *Annals of the Association of American Geographers*, *92*, 241–266.

Long, H., & Zhao, Z. M. (2005). Urban road extraction from high-resolution optical satellite images. *International Journal of Remote Sensing*, *26*(22), 4907–4921.

Lu, D., Tian, H., Zhou, G., & Ge, H. (2008). Regional mapping of human settlements in southeastern China with multisensor remotely sensed data. *Remote Sensing of Environment*, *112*(9), 3668–3679.

Lu, D., & Weng, Q. (2004). Spectral mixture analysis of the urban landscape in Indianapolis with Landsat ETM+ imagery. *Photogrammetric Engineering and Remote Sensing*, *70*, 1053–1062.

Lu, D., & Weng, Q. (2005). Urban land-use and land-cover mapping using the full spectral information of Landsat ETM+ data in Indianapolis, Indiana. *Photogrammetric Engineering and Remote Sensing*, *71*(11), 1275–1284.

Lu, D., & Weng, Q. (2006). Use of impervious surface in urban land use classification. *Remote Sensing of Environment*, *102*(1–2), 146–160.

Lu, D., & Weng, Q. (2007). A survey of image classification methods and techniques for improving classification performance. *International Journal of Remote Sensing*, *28* (5), 823–870.

Lu, D., & Weng, Q. (2009). Extraction of urban impervious surfaces from IKONOS imagery. *International Journal of Remote Sensing*, *30*(5), 1297–1311.

Lu, D., Hetrick, S., & Moran, E. in press. Impervious surface mapping with Quickbird imagery. International Journal of Remote Sensing. doi:10.1080/01431161003698393.

Luo, R. C., & Kay, M. G. (1989). Multisensor integration and fusion for intelligent systems. *IEEE Transactions on Systems, Man, and Cybernetics*, *19*, 901–931.

Luo, L., & Mountrakis, G. (2010). Integrating intermediate inputs from partially classified images within a hybrid classification framework: An impervious surface estimation example. *Remote Sensing of Environment*, *114*, 1220–1229.

Madhavan, B. B., Kubo, S., Kurisaki, N., & Sivakumar, T. V. L. N. (2001). Appraising the anatomy and spatial growth of the Bangkok Metropolitan area using a vegetation–impervious–soil model through remote sensing. *International Journal of Remote Sensing*, *22*, 789–806.

Magnussen, S., Boudewyn, P., & Wulder, M. (2004). Contextual classification of Landsat TM images to forest inventory cover types. *International Journal of Remote Sensing*, *25*, 2421–2440.

Mannan, B., & Ray, A. K. (2003). Crisp and fuzzy competitive learning networks for supervised classification of multispectral IRS scenes. *International Journal of Remote Sensing*, *24*, 3491–3502.

Mather, P. M. (1999). Land cover classification revisited. In P. M. Atkinson, & N. J. Tate (Eds.), *Advances in Remote Sensing and GIS* (pp. 7–16). New York: John Wiley & Sons.

Mayer, H. (1999). Automatic object extraction from aerial imagery — A survey focusing on building. *Computer Vision and Image Understanding*, *74*(2), 138–139.

McGwire, K., Minor, T., & Fenstermaker, L. (2000). Hyperspectral mixture modeling for quantifying sparse vegetation cover in arid environments. *Remote Sensing of Environment*, *72*, 360–374.

Mena, J. B. (2003). State of the art on automatic road extraction for GIS update: A novel classification. *Pattern Recognition Letters*, *24*(16), 3037–3058.

Miliaresis, G., & Kokkas, N. (2007). Segmentation and object-based classification for the extraction of the building class from LiDAR DEMs. *Computers and Geosciences*, *33* (8), 1076–1087.

Mohapatra, R. P., & Wu, C. (2007). Subpixel imperviousness estimation with IKONOS imagery: An Artificial Neural Network approach. In Q. Weng (Ed.), *Remote Sensing of Impervious Surfaces* (pp. 21–37). Boca Raton, FL: CRC Press.

Moons, T., Frère, D., Vandekerckhove, J., & Van Gool, L. (1998). Automatic modeling and 3D reconstruction of urban house roofs from high resolution aerial imagery. *Proceedings Of Fifth European Conference On Computer Vision I* (pp. 410–425).

Moses, W. J., Gitelson, A. A., Berdnikov, S., & Povazhnyy, V. (2009). Satellite estimation of Chlorophyll-a concentration using the red and NIR bands of MERIS—The Azov Sea case study. *IEEE Geoscience and Remote Sensing Letters*, *6*, 845–849.

Myint, S. W. (2001). A robust texture analysis and classification approach for urban land-use and land-cover feature discrimination. *Geocarto International*, *16*, 27–38.

National Research Council (2007). *Earth science and applications from space: National imperatives for the next decade and beyond*. Washington, DC: The National Academy Press.

Pal, N. R., Laha, A., & Das, J. (2005). Designing fuzzy rule based classifier using self-organizing feature map for analysis of multispectral satellite images. *International Journal of Remote Sensing*, *26*(10), 2219–2240.

Pal, M., & Mather, P. M. (2003). An assessment of the effectiveness of decision tree methods for land cover classification. *Remote Sensing of Environment*, *86*, 554–565.

Pal, N. R., & Pal, S. K. (1993). A review on image segmentation techniques. *Pattern Recognition*, *26*(9), 1277–1294.

Paola, J. D., & Schowengerdt, R. A. (1995). A review and analysis of back propagation neural networks for classification of remotely sensed multispectral imagery. *International Journal of Remote Sensing*, *16*, 3033–3058.

Peteri, R., & Ranchin, T. (2007). Road networks derived from high spatial resolution satellite remote sensing data. In Q. Weng (Ed.), *Remote Sensing of Impervious Surfaces* (pp. 215–236). Boca Raton, Florida: CRC Press.

Phinn, S. R. (1998). A framework for selecting appropriate remotely sensed data dimensions for environmental monitoring and management. *International Journal of Remote Sensing*, *19*, 3457–3463.

Phinn, S. R., Menges, C., Hill, G. J. E., & Stanford, M. (2000). Optimizing remotely sensed solutions for monitoring, modeling, and managing coastal environments. *Remote Sensing of Environment*, *73*, 117–132.

Phinn, S., Stanford, M., Scarth, P., Murray, A. T., & Shyy, P. T. (2002). Monitoring the composition of urban environments based on the vegetation–impervious surface–soil (VIS) model by subpixel analysis techniques. *International Journal of Remote Sensing*, *23*, 4131–4153.

Platt, R. V., & Goetz, A. F. H. (2004). A comparison of AVIRIS and Landsat for land use classification at the urban fringe. *Photogrammetric Engineering and Remote Sensing*, *70*, 813–819.

Pohl, C., & van Genderen, J. L. (1998). Multisensor image fusion in remote sensing: Concepts, methods, and applications. *International Journal of Remote Sensing*, *19*, 823–854.

Powell, S. L., Cohen, W. B., Yang, Z., Pierce, J. D., & Alberti, M. (2008). Quantification of impervious surface in the Snohomish Water Resources Inventory Area of Western Washington from 1972–2006. *Remote Sensing of Environment*, *112*, 1895–1908.

Powell, R. L., Roberts, D. A., Dennison, P. E., & Hess, L. L. (2007). Sub-pixel mapping of urban land cover using multiple endmember spectral mixture analysis: Manaus, Brazil. *Remote Sensing of Environment*, *106*(2), 253–267.

Pu, R., Kelly, M., Anderson, G. L., & Gong, P. (2008). Using CASI hyperspectral imagery to detect mortality and vegetation stress associated with a new hardwood forest disease. *Photogrammetric Engineering and Remote Sensing*, *74*(1), 65–75.

Quattrochi, D. A., & Goodchild, M. F. (1997). *Scale in remote sensing and GIS*. New York City, NY: Lewis Publishers.

Rashed, T., Weeks, J. R., Roberts, D., Rogan, J., & Powell, R. (2003). Measuring the physical composition of urban morphology using multiple endmember spectral mixture models. *Photogrammetric Engineering and Remote Sensing*, *69*, 1011–1020.

Ridd, M. K. (1995). Exploring a V–I–S (Vegetation–Impervious Surface–Soil) model for urban ecosystem analysis through remote sensing: Comparative anatomy for cities. *International Journal of Remote Sensing*, *16*(12), 2165–2185.

Roberts, D. A., Batista, G. T., Pereira, J. L. G., Waller, E. K., & Nelson, B. W. (1998). Change identification using multitemporal spectral mixture analysis: Applications in eastern Amazônia. In R. S. Lunetta, & C. D. Elvidge (Eds.), *Remote sensing change detection: Environmental monitoring methods and applications* (pp. 137–161). Ann Arbor, MI: Ann Arbor Press.

Roberts, D. A., Gardner, M., Church, R., Ustin, S., Scheer, G., & Green, R. O. (1998). Mapping chaparral in the Santa Monica mountains using multiple endmember spectral mixture models. *Remote Sensing of Environment*, *65*, 267–279.

Samadzadegan, F., Bigdeli, B., & Hahn, M. (2009). Automatic road extraction from LIDAR data based on classifier fusion in urban area. *2009 Joint Urban Remote Sensing Event* (pp. 1–6). doi:10.1109/URS.2009.5137739.

Schmidt, K. S., Skidmore, A. K., Kloosterman, E. H., van Oosten, H., Kumar, L., & Janssen, J.A.M. (2004). Mapping coastal vegetation using an expert system and hyperspectral imagery. *Photogrammetric Engineering and Remote Sensing*, *70*, 703–715.

Schneider, A., Friedl, M. A., & Potere, D. (2010). Mapping global urban areas using MODIS 500-m data: New methods and datasets based on 'urban ecoregions'. *Remote Sensing of Environment*, *114*, 1733–1746.

Schueler, T. R. (1994). The importance of imperviousness. *Watershed Protection Techniques*, *1*, 100–111.

Setiawan, H., Mathieu, R., & Thompson-Fawcett, M. (2006). Assessing the applicability of the V–I–S model to map urban land use in the developing world: Case study of Yogyakarta, Indonesia. *Computers, Environment and Urban Systems*, *30*(4), 503–522.

Shaban, M. A., & Dikshit, O. (2001). Improvement of classification in urban areas by the use of textural features: The case study of Lucknow City, Uttar Pradesh. *International Journal of Remote Sensing*, *22*, 565–593.

Sharma, K. M. S., & Sarkar, A. (1998). A modified contextual classification technique for remote sensing data. *Photogrammetric Engineering and Remote Sensing*, *64*(4), 273–280.

Shi, W. Z., & Zhu, C. Q. (2002). The line segment match method for extracting road network from high-resolution satellite images. *IEEE Transactions on Geoscience and Remote Sensing*, *40*(2), 511–514.

Slonecker, E. T., Jennings, D., & Garofalo, D. (2001). Remote sensing of impervious surface: A review. *Remote Sensing Reviews*, *20*, 227–255.

Soil Conservation Service (1975). *Urban hydrology for small watersheds, USDA Soil Conservation Service Technical Release No. 55*. Washington, DC: U.S. Department of Agriculture.

Solberg, A. H. S., Taxt, T., & Jain, A. K. (1996). A Markov random field model for classification of multisource satellite imagery. *IEEE Transactions on Geoscience and Remote Sensing*, *34*, 100–112.

Stefanov, W. L., Ramsey, M. S., & Christensen, P. R. (2001). Monitoring urban land cover change: an expert system approach to land cover classification of semiarid to arid urban centers. *Remote Sensing of Environment*, *77*, 173–185.

Stow, D., Coulter, L., Kaiser, J., Hope, A., Service, D., Schutte, K., et al. (2003). Irrigated vegetation assessment for urban environments. *Photogrammetric Engineering and Remote Sensing*, *69*, 381–390.

Strahler, A. H., Woodcock, C. E., & Smith, J. A. (1986). On the nature of models in remote sensing. *Remote Sensing of Environment*, *70*, 121–139.

Stuckens, J., Coppin, P. R., & Bauer, M. E. (2000). Integrating contextual information with per-pixel classification for improved land cover classification. *Remote Sensing of Environment*, *71*, 282–296.

Tan, Q., Liu, Z., & Li, X. (2009). Mapping urban surface imperviousness using SPOT multispectral satellite images. *Proceedings of IEEE Geoscience and Remote Sensing Symposium (IGARSS 2009), III-346 - III-348, Cape Town.* doi:10.1109/IGARSS.2009.5417773.

Thenkabail, P. S., Enclona, E. A., Ashton, M. S., Legg, C., & de Dieu, M. J. (2004a). Hyperion, IKONOS, ALI, and ETM+ sensors in the study of African rainforests. *Remote Sensing of Environment*, *90*, 23–43.

Thenkabail, P. S., Enclona, E. A., Ashton, M. S., & van der Meer, B. (2004b). Accuracy assessments of hyperspectral waveband performance for vegetation analysis applications. *Remote Sensing of Environment*, *91*, 354–376.

Tiwari, P. S., Pande, H., & Pandey, A. K. (2009). Automatic urban road extraction using airborne laser scanning/altimetry and high resolution satellite data. *Journal of the Indian Society of Remote Sensing*, *37*(2), 223–231. doi:10.1007/s12524-009-0023-9.

Tong, X., Liu, S., & Weng, Q. (2009). Geometric processing of Quickbird stereo imagery for urban land use mapping — A case study in Shanghai, China. *IEEE Journal of Selected Topics in Applied Earth Observations & Remote Sensing*, *2*(2), 61–66.

Tullis, J. A., & Jensen, J. R. (2003). Export system house detection in high spatial resolution imagery using size, shape, and context. *Geocarto International*, *18*, 5–15.

Turner, B. L. I. I., Skole, D., Sanderson, S., Fisher, G., Fresco, L., & Leemans, R. (1995). *Land-use and land-cover change: Science and research plan.* Stockhdm and Geneva: International Geosphere-Bioshere Program and the Human Dimensions of Global Environmental Change Programme (IGBP Report No. 35 and HDP Report No. 7).

van der Linden, S., & Hostert, P. (2009). The influence of urban structures on impervious surface maps from airborne hyperspectral data. *Remote Sensing of Environment*, *113*, 2298–2305.

Van de Voore, T., De Genst, W., Canters, F., Stephenne, N., Wolff, E., & Binnard, M. (2003). Extraction of land use/land cover — Related information from very high resolution data in urban and suburban areas. *Proceedings of the 23 rd Symposium of the European Association of Remote Sensing Laboratories* (pp. 237–244).

Wang, F. (1990). Fuzzy supervised classification of remote sensing images. *IEEE Transactions on Geoscience and Remote Sensing*, *28*(2), 194–201.

Wang, L., Sousa, W. P., Gong, P., & Biging, G. S. (2004). Comparison of IKONOS and QuickBird images for mapping mangrove species on the Caribbean coast of panama. *Remote Sensing of Environment*, *91*, 432–440.

Ward, D., Phinn, S. R., & Murray, A. T. (2000). Monitoring growth in rapidly urbanizing areas using remotely sensed data. *The Professional Geographer*, *53*, 371–386.

Weng, Q. (2001). Modeling urban growth effect on surface runoff with the integration of remote sensing and GIS. *Environmental Management*, *28*, 737–748.

Weng, Q. (2007). *Remote sensing of impervious surfaces* (pp. xv–xxvii). Boca Raton, FL: CRC Press.

Weng, Q. (2009). Remote sensing and GIS integration: Theories, methods, and applications. New York: McGraw-Hill.

Weng, Q., & Hu, X. (2008). Medium spatial resolution satellite imagery for estimating and mapping urban impervious surfaces using LSMA and ANN. *IEEE Transaction on Geosciences and Remote Sensing*, *46*(8), 2397–2406.

Weng, Q., Hu, X., & Liu, H. (2009). Estimating impervious surfaces using linear spectral mixture analysis with multi-temporal ASTER images. *International Journal of Remote Sensing*, *30*(18), 4807–4830.

Weng, Q., Hu, X., & Lu, D. (2008). Extracting impervious surface from medium spatial resolution multispectral and hyperspectral imagery: A comparison. *International Journal of Remote Sensing*, *29*(11), 3209–3232.

Weng, Q., & Lu, D. (2009). Landscape as a continuum: An examination of the urban landscape structures and dynamics of Indianapolis city, 1991–2000. *International Journal of Remote Sensing*, *30*(10), 2547–2577.

Wu, C. (2004). Normalized spectral mixture analysis for monitoring urban composition using ETM+ imagery. *Remote Sensing of Environment*, *93*, 480–492.

Wu, C. (2009). Quantifying high-resolution impervious surfaces using spectral mixture analysis. *International Journal of Remote Sensing*, *30*(11), 2915–2932.

Wu, C., & Murray, A. T. (2003). Estimating impervious surface distribution by spectral mixture analysis. *Remote Sensing of Environment*, *84*, 493–505.

Xian, G. (2007). Mapping impervious surfaces using classification and regression tree algorithm. In Q. Weng (Ed.), *Remote Sensing of Impervious Surfaces* (pp. 39–58). Boca Rotan, FL: CRC Press.

Yang, L., Huang, C., Homer, C. G., Wylie, B. K., & Coan, M. J. (2003). An approach for mapping large-scale impervious surfaces: Synergistic use of Landsat-7 ETM+ and high spatial resolution imagery. *Canadian Journal of Remote Sensing*, *29*, 230–240.

Yang, L., Jiang, L., Lin, H., & Liao, M. (2009). Quantifying sub-pixel urban impervious surface through fusion of optical and InSAR imagery. *GIScience & Remote Sensing*, *46*(2), 161–171.

Yang, F., Matsushita, B., & Fukushima, T. (2010). A pre-screened and normalized multiple endmember spectral mixture analysis for mapping impervious surface area in Lake Kasumigaura Basin, Japan. *ISPRS Journal of Photogrammetry and Remote Sensing*, *65*, 479–490.

Yu, B., Liu, H., Wu, J., Hu, Y., & Zhang, L. (2010). Automated derivation of urban building density information using airborne LiDAR data and object-based method. *Landscape and Urban Planning*, *98*(3–4), 210–219.

Yuan, F., & Bauer, M. E. (2006). Mapping impervious surface area using high resolution imagery: A comparison of object-based and per pixel classification. *American Society for Photogrammetry and Remote Sensing Annual Conference Proceedings, Reno, Nevada* (unpaginated).

Yuan, F., Wu, C., & Bauer, M. E. (2008). Comparison of spectral analysis techniques for impervious surface estimation using Landsat imagery. *Photogrammetric Engineering and Remote Sensing*, *74*(8), 1045–1055.

Zhou, G. Q., & Kelmelis, J. A. (2006). True orthoimage generation for urban areas with very buildings. In Q. Weng, & D. A. Quattrochi (Eds.), *Urban Remote Sensing* (pp. 3–20). Boca Raton, FL: CRC Press.

Zhou, W., & Troy, A. (2008). An object-oriented approach for analyzing and characterizing urban landscape at the parcel level. *International Journal of Remote Sensing*, *29*(11), 3119–3135.

Zhou, Y. Y., & Wang, Y. Q. (2008). Extraction of impervious, surface areas from high spatial resolution imagery by multiple agent segmentation and classification. *Photogrammetric Engineering and Remote Sensing*, *74*(7), 857–868.

Zhu, C., Shi, W., Pesaresi, M., Liu, L., Chen, X., & King, B. (2005). The recognition of road network from high-resolution satellite remotely sensed data using image morphological characteristics. *International Journal of Remote Sensing*, *26*(24), 5493–5508.